

UNIVERSIDAD SAN FRANCISCO DE QUITO USFQ

Colegio de Posgrados

**Flowmetry and Micrometric Imaging using Optical Feedback
Interferometry (OFI)**

Denis Michael Flores Pazos

**Julien Perchoux Ph.D
Director de Trabajo de Titulación**

Trabajo de titulación de posgrado presentado como requisito
para la obtención del título de Magister en Nanoelectrónica

Quito, 13 de diciembre de 2019

UNIVERSIDAD SAN FRANCISCO DE QUITO USFQ**COLEGIO DE POSGRADOS****HOJA DE APROBACIÓN DE TRABAJO DE TITULACIÓN****Flowmetry and Micrometric Imaging using Optical Feedback
Interferometry (OFI)****Denis Michael Flores Pazos**

Firmas

Julien Perchoux, PhD.

Director Máster ESECA, Toulouse, Francia



Omar Aguirre, PhD.

Director de la Maestría en Nanoelectrónica

César Zambrano, PhD.

Decano del Colegio de Ciencias e
Ingenierías

Hugo Burgos, PhD.

Decano del Colegio de Posgrados

Quito, 13 de diciembre de 2019

© Derechos de Autor

Por medio del presente documento certifico que he leído todas las Políticas y Manuales de la Universidad San Francisco de Quito USFQ, incluyendo la Política de Propiedad Intelectual USFQ, y estoy de acuerdo con su contenido, por lo que los derechos de propiedad intelectual del presente trabajo quedan sujetos a lo dispuesto en esas Políticas.

Asimismo, autorizo a la USFQ para que realice la digitalización y publicación de este trabajo en el repositorio virtual, de conformidad a lo dispuesto en el Art. 144 de la Ley Orgánica de Educación Superior.

Firma:



Nombre:

Denis Michael Flores Pazos

Código de estudiante:

00203885

C. I.:

1719895771

Lugar, Fecha

Quito, 13 de diciembre de 2019

DEDICATORIA

Dedico el presente trabajo a mi familia, en especial a mi madre Graciela quien, con amor, esfuerzo, apoyo y orientación ha logrado inculcar en mi la determinación de alcanzar mis objetivos, disciplina y dedicación frente a cada desafío afrontado, a mi hermano Marco por su ayuda, consejos y preocupación en todo momento recordándome siempre el camino del bien y los lazos familiares, a mi novia Lëann quien, con su amor, apoyo, compañía y valor me ha permitido sentirme en casa incluso en un lugar tan lejano de mi país, y mantener la firmeza frente a toda situación. A mis amigos porque siempre hemos estado pendientes de cada uno de nuestros problemas y victorias suscitadas a lo largo de la vida, por brindarme su preocupación y motivación la cual valoro y valoraré siempre.

Denis Flores

AGRADECIMIENTOS

A mi querida Universidad San Francisco de Quito USFQ y el Institut National Polytechnique de Toulouse por haber sido lugares donde desarrollé y mejoré muchos conocimientos, actitudes profesionales e investigativas que me han permitido culminar mis estudios de master, conocer excelentes personas y haberme inculcado valores de responsabilidad y ética profesional.

Al doctor Lionel Trojman por ser el pionero y dar su esfuerzo y tiempo en la construcción del programa de master en nanoelectrónica, el único en Ecuador, y por su dedicación a que este se desarrolle de manera satisfactoria con alta calidad.

Al doctor Julien Perchoux por brindarme y ayudarme su conocimiento y consejo en mi etapa de pasantías en LAAS-CNRS, además de guiar y encaminar los estudios del Master ESECA en el Institut Polytechnique National de Toulouse – ENSEEIHT en Francia, y por abrir las puertas a la colaboración bilateral con la USFQ para este programa de maestría.

Al doctor Adam Quotb por su calidad como profesor y apoyo excepcional durante todo el programa del master en Francia, por darme la oportunidad de realizar mis pasantías en LAAS-CNRS y confiar en mi para la realización y colaboración en la investigación científica en el equipo OSE.

A mi familia, mi novia, amigos y compañeros por estar conmigo apoyándome a lo largo de esta etapa y por seguir haciéndolo en las venideras, que con su ayuda he logrado grandes metas en mi formación personal y profesional.

RESUMEN

Los sistemas optoelectrónicos están presentes en la mayoría de sensores y dispositivos electrónicos utilizados en la actualidad. Dado el incremento continuo de la tecnología biomédica que pretende el mejoramiento e innovación de dispositivos con fines médicos para no solo el tratamiento de enfermedades, sino también su estudio.

Dicho estudio ayuda a los médicos y especialistas al entendimiento de cómo interactúan las enfermedades y fenómenos dentro del cuerpo humano y como deben ser analizadas y tratadas.

En este contexto, este trabajo se centra en el campo de los micro fluidos, el cual se dedica mayormente al entendimiento de partículas y células dentro del torrente sanguíneo, piel, y tejidos.

Muchas tecnologías actuales permiten la identificación de partículas y su caracterización en el campo de los micro fluidos, sin embargo, muchos requieren de tecnologías complejas y por ende costosas, generando así una inaccesibilidad por parte de todas las clases sociales a ciertos estudios y tratamientos médicos, tomando especial consideración en esta limitante, mediante la tecnología de interferometría láser, este trabajo pretende mejorar esta técnica en sentidos económicos y de compactibilidad.

Finalmente se logró un gran avance y una publicación científica en el congreso IEEE Sensors 2019 mediante la inclusión de la técnica de escaneo continuo, innovando y abriendo el camino a nuevos estudios para continuar el desarrollo de esta técnica.

Palabras clave: Optoelectrónica, Biomedicina, Microfluidos, Interferometría láser.

ABSTRACT

Optoelectronic systems are present in most electronic sensors and devices used today. Given the continuous increase in biomedical technology that aims to improve and innovate devices for medical purposes for not only the treatment of diseases, but also their study.

This study helps doctors and specialists to understand how diseases and phenomena interact within the human body and how they should be analyzed and treated.

In this context, this work focuses on the field of micro fluids, which is mainly dedicated to the understanding of particles and cells within the bloodstream, skin, and tissues.

Many current technologies allow the identification of particles and their characterization in the field of micro fluids, however, many require complex and therefore expensive technologies, thus generating an inaccessibility by all social classes to certain medical studies and treatments, taking special consideration in this limitation, using laser interferometry technology, this work aims to improve this technique in economic and compactness senses.

Finally, a great advance and a scientific publication were achieved at the IEEE Sensors 2019 congress by including the continuous scanning technique, innovating and opening the way to new studies to continue the development of this technique.

Key words: Optoelectronics, Biomedics, Microfluidics, Laser Interferometry.

TABLA DE CONTENIDO

Resumen	6
Abstract.....	7
INTRODUCTION.....	13
STATE OF THE ART	16
CHAPTER 1	18
OPTICAL FEEDBACK INTERFEROMETRY IN MICROFLUIDICS	18
1.1 Optical Feedback Interferometry (OFI).....	18
1.2 Optical Feedback Interferometry in Fluidics Sensing	20
1.3 The Scattering Regimes	21
1.4 Flowmetry using OFI.....	22
1.4.1 OFI for Flowmetry.....	22
1.4.2 OFI Flowmetry Methods.	23
1.5 OFI for Flow Imaging.....	25
CHAPTER 2	26
OFI FLOW DETECTION	26
2.1 Experimental Set-Up.....	26
2.1.1 Microfluidic Channel.	26
2.1.2 Electronic System Scheme.	27
2.1.3 Hydrodynamic Supply System.	28
2.1.4 Displacement System.	30
2.2 Acquisition Logic and Continuous Scanning Improvement.....	31
2.3 Signal Processing and Microchannel Algorithm Recognition	32
2.4 Results.....	37
CHAPTER 3	46
OFI IMAGING SYSTEMS FOR MICROMETRIC FLOW-PATTERNS.....	46
3.1 OFI Imaging System using a three axis displacement System.....	46
3.1.1 Experimental Set-Up.....	46
3.1.2 Signal Processing and Continuous Scanning Integration.....	48
3.1.3 Results.	51

3.2 OFI Imaging System using Mirror Beam Steering	58
3.2.1 Experimental Set-Up.....	58
3.2.2 Beam Steer Mirror Command and Data Acquisition Algorithm.	66
3.2.3 Results.	71
CONCLUSIONS.....	75
REFERENCES.....	76
ÍNDICE DE ANEXOS.....	78
ANEXO A: MATLAB® Graphic user interface code	78
ANEXO B: MATLAB® Fuctions for Zaber-Tech Stepper Control.....	94
ANEXO C: MATLAB® Acquisition Signal Event	96
ANEXO D: MATLAB® Code for Handheld Device Control	97
ANEXO E: MATLAB® Code for Imaging Construction.....	99

ÍNDICE DE TABLAS

Table 1. Description of the graphic interface developed.	36
Table 2. Minimum parameters obtained with the NI USB-6361.	68
Table 3. Distance Limits controlled by continuous scanning axis.	69

ÍNDICE DE FIGURAS

Figure 1. Optical Feedback Interferometry Scheme [15].....	19
Figure 2. Schematic of OFI applied to fluid flow profile measurement [1], [17].....	20
Figure 3. Light scattering with particles embedded in a fluid. The light (yellow) is scattered by more than one particle [19].....	22
Figure 4. PDMS circular micrometric fluidic channel.....	26
Figure 5. PDMS microfluidic channel, with laser scheme using two lenses.....	28
Figure 6. Hydrodynamic Supply System.....	29
Figure 7. 3 Axis (XYZ) Displacement System Configuration.....	30
Figure 8. Algorithm Logic Flow Diagram.....	32
Figure 9. Signal Processing Algorithm Flow Diagram.....	34
Figure 10. Graphic User Interface Created to perform data Acquisition.....	35
Figure 11. Microchannel dimension and volumetric flow rate.....	38
Figure 12. OFI signals fluctuations at different speed of the displacement system.....	39
Figure 13. Different OFI signals in time domain.....	40
Figure 14. Laser Scanning direction, before and after microchannel (Upper View).....	41
Figure 15. Fluctuation range detection of OFI signals in time domain.....	42
Figure 16. Power Spectrum of the OFI signals according to different proximities.....	43
Figure 17. Zeroth and First Moments of the Power Spectral Signals.....	44
Figure 18. Measurement signal after entering the coordinates in the middle of the channel...	45
Figure 19. Experimental Configuration Diagram (a) Front view and (b) Upper view.....	47
Figure 20. Photo-lithographic Microfluidic Chip (Serpentine form) and tilted angle.....	47
Figure 21. Microfluidic chip support for flow supplying.....	48
Figure 22. Flow Diagram correspondent to the measurements and signal processing.....	50
Figure 23. Image of all serpentine (a) Vertical scanning (25 $\mu\text{m}/\text{pixel}$ x 10 $\mu\text{m}/\text{pixel}$, total 608x1137 pixels Horizontal X Vertical), (b) Horizontal Scanning (10 $\mu\text{m}/\text{pixel}$ x 50 $\mu\text{m}/\text{pixel}$, total 800x214 pixels).....	52
Figure 24. Single Channel Measurement over the Serpentine Piece, with 200 samples along the vertical axis (a) Flow concentration, (b) power spectrum of flow and no flow sections	54

Figure 25. Power contributions with (a) motor displacement with empty and full of fluid channel, and (b) flowing fluid with displacement and without it.....	55
Figure 26. Section Image over the Serpentine (1 $\mu\text{m}/\text{pixel}$ x 10 $\mu\text{m}/\text{pixel}$) (4000x1097 pixels) (a) Milk dilution at 10 $\mu\text{L}/\text{min}$, (b) Steady milk (no Flow), (c) Subtraction between (a) and (b) consonant to flow pattern.....	56
Figure 27. Diagnostics OFI Sensor with it handheld device and metallic base [3].	60
Figure 28. (a) Laser Diode and (b) Conditioning Circuit PCB placed in the handheld System.	61
Figure 29. Optical 2D Scanning System Embedded in the handheld device [3].	62
Figure 30. Mount-DIP.5-KMS PCB Connector.....	63
Figure 31. Control Voltage Vs Tilt Degree of the Mirror produced by the BDQ Driver.	64
Figure 32. Handheld Device interior with placement of Beam steering mirror, PCB connector and BDQ driver.	65
Figure 33. Base interior with the Data Acquisition Board and Power Supply.....	66
Figure 34. Flow Diagram of the Initialization Sequence of the Mirrorcle S4417.	67
Figure 35. Flow diagram of the entire procedure for control and acquisition of the system. ..	71
Figure 36. Focusing Over the Serpentine Chip using the Handheld System.	72
Figure 37. First measurements over the serpentine chip (a) small section of the microchannel with a fixed step of 20 μm and a segmentation step of 10 μm	73
Figure 38. Section of the Serpentine taken with vertical Scanning.	74

INTRODUCTION

The optoelectronic systems are in continuous evolution and their applications nowadays could be found in several disciplines, like it is the case of the Microfluidics, where we can encounter applications related to biomedical engineering, physics, chemistry, biochemistry, nanotechnology and biotechnology [1].

In the field of the biomedical engineering, most of the topics treated are focused in microvascular, blood perfusion and cytometry. All of these require high accuracy in the measurements and pursue the goal to be non-invasive for the future development of powerful and helpful instruments to diagnose, analyze and treat deceases [2].

In this context, the microfluidics became a discipline worth to develop in order to reach technologies which contributes to the biomedical field. All these requirements and features could be easy to achieve using the advantages of the optoelectronics systems. The combination between both are being developed and studied for applications like biosensors, lab-on-chip devices, lenses, molecular imaging and energy, etc. This technology is also called “Optofluidics” [3] [4].

Within the Optoelectronics there are several techniques which constantly has been improved according its applications. One of these is the interferometry, which nowadays is well-stablished and useful both in research and industry. Usually the set-up for each interferometer differs, and the most common are the Michelson, Mach-Zehnder, Sagnac and Fabry-Perot Interferometer [1].

Optical Feedback Interferometry (OFI) or Self-Mixing Interferometry (SMI) is a technique to achieve an interferometric pattern with a different approach from what is usually done. It consists in re-injecting the laser light reflected by and external object into the laser

cavity where it interferes, non-linearly with the light already present inside the cavity [2], [5]–[7].

The OFI technology is attractive due to its features such as non-invasiveness, non-destructiveness, compactness, simplicity, low cost, self-alignment, etc. Within the interferometric techniques, OFI is likely to be the most compact of all, and its design offer the possibility to achieve embedded systems and tools in several disciplines like is the case of the microfluidics domain [6]–[8].

However, OFI sensing performance requires to be upgraded until it became equal like the case of Laser Doppler Velocimetry (LDV) and micro Particle Image Velocimetry technologies which already has been accepted like the standards for industry and research. New OFI sensors always take in consideration this purpose to contribute the improvement of the sensing approach [3].

The OFI technique is currently being improved and researchers constantly find new applications where it is worth to focus, develop their models and polish their set-ups, like it is the case of the Laboratory for Analysis and Architecture of Systems (LAAS-CNRS) in France, where its research group of Optoelectronics for Embedded Systems (OSE) every day enhance this technology and its applications in development.

This internship topic was involved in this context of the use of the laser sensing techniques based on the Optical Feedback Interferometry (OFI) technology for flowmetry and imaging at micro-scale applications. These studies and deeds could be performed in the LAAS facilities where all the features using OFI technology have been taking in advantage in order to obtain results with good performance.

This manuscript is organized in a way that first is explained the fundamentals of OFI and it use to perform microfluidic applications such is the case of flowmetry and imaging systems,

and then there are detailed the two main experimental phases which are: Flow detection and micro-metric imaging system using two different configurations.

STATE OF THE ART

This internship work is a direct continuation of the previous PhD students who focus their thesis subjects in the microfluidic systems and flowmetry study using Optical Feedback Interferometry and also the research and projects accorded to this of the OSE Group at LASS-CNRS. The directives during the internship were focused in three different subjects.

The first problematic is focused in the flow detection using high particle concentration in a single channel. In the previous works [2], [3], [17], a single channel where the fluid at high concentration of particles is flowing is used in this task. Using a three axis displacement system the laser focusing over the channel was done while a data acquisition system such a data acquisition board or an oscilloscope is used to monitor the OFI signal. This process is done manually by commanding the position of the displacement system.

Ramirez Miquet [22], da Costa Moreira [3] and Campagnolo [23] during their experiments in order to perform flow detection and measurement used motorized displacement systems which could be commanded manually by a graphical interface and using a data acquisition board which measure the signal and obtain the power spectrum simultaneously, find the optimal point of focus which correspond to the center of the microchannel.

Based in this context the first stage was to develop an algorithm which can make the automatic detection of the microchannel, and thus replacing the manual system that although it is simple, several times could take more time since depending the laser wavelength, we could have the visual contact of the target or not. By obtaining this the detection we can automate the process of centering in the microchannel to then perform the flow characterization.

The second problematic during this work, was concerned the imaging systems using the OFI sensing technique. Previous works have already proposed laser Doppler systems based on the OFI sensing scheme [5]–[7], [22]. But, so far, the flow detection was done by moving the

scanning system step by step in two dimensions over the area of interest to reproduce the image. At each position, several samples were acquired, resulting in long dead times and whereby the trade-off between acquisition time and image quality generally result in images that require hours of acquisition.

The proposition of Kliese et al [24] establish a quick scan system where the OFI signal is being acquired at 100 KHz and at the same time while the displacement is performed along a line of interest at 1 mm/s. Resulting in a good recognition of the flow concentration using the spectrogram. This mark the starting point to use this technique for develop rasterization systems where we can improve the time of acquisition.

The improvement has two stages during this work, at first there is proposed a motorized displacement system which allow the continuous scanning with two degrees of freedom, in order to experiment with the different directions that could be used. With this approach we expect to improve the acquisition time and still keep a good resolution. The second stage proposed is to reproduce the same results using an embedded electronic system which replaces this translation system, and by this way obtain a suitable system for biomedical applications such is the case of the blood perfusion.

For the IEEE sensors conference 2016, da Costa Morerira et al [7] proposed an embedded imaging system using a micro-electro-mechanical system (MEMS), much smaller than the motorized displacement system, and that take advantages of the compactness of it combined with the OFI sensing scheme.

CHAPTER 1

OPTICAL FEEDBACK INTERFEROMETRY IN MICROFLUIDICS

1.1 Optical Feedback Interferometry (OFI)

Optical feedback has been studied since the invention of the laser, the first demonstration of its existence was done by Kleinman and Kisliuk in 1962, however, it was considered as a parasitic effect which affects both laser's frequency and amplitude. It was until 1963 when it was demonstrated by King and Steward, that it has potential capabilities in sensing applications. [9]. They filed a patent application that introduced a general discussion on the potential of OFI for measuring physical parameters [10].

During the sixties, the arrangements were studied and improved to avoid the external feedback entering back in the resonant cavity of the laser, although, in 1968, Rudd proposed the first Doppler velocimeter using OFI in He-Ne gas laser [11]. Gas lasers was used and improved during the seventies until the eighties when OFI started to be implemented in sensors which implement the semiconductor technology. In 1980, Lang and Kobayashi studied the phenomenon of external feedback in laser diodes and developed the equations which rule their behavior, their model until today in most of the applications represents the keystone on describing the laser dynamics under feedback [12].

Nevertheless, there exists the "Three mirror model" which describes the laser under optical feedback as a three mirrors Fabry-Perot cavity. A geometrical analysis allow the study of stationary waves supported by the system and how the laser modes depend of the external feedback [13]. In other words, here the target works as a third mirror. This is useful to have a

schematic idea of what happens into the laser cavity, additionally allow the better understand of the physics behind the equations.

The optical feedback effect due to a laser light, also called self-mixing effect, happens when part of the light from the laser beam, which is scattered from an external target, is re-injected into its cavity, where it interference. Nowadays, this effect is used to characterize and obtain as many information as possible about the target that we are focusing. [3]

OFI results from the interference produced inside the laser diode cavity, where the electromagnetic wave emitted and the wave that is back-scattered or reflected by a distant target collide and produce a non-linear superposition of its fields. This interference leads to variations of the output power and frequency of the laser beam, which contains the information related to the target. [7].

In this way the laser became at the same time, the source and the detector of the optical system, and no external detector are needed since it is done conventionally. Even so, sometimes the alignment procedure between the laser and the external reflector is necessary. The ratio between the feedback and the emitted power is in the order of 10^{-8} , which allow that the measures on extremely low reflective materials or rough surfaces could be made [2], [14].

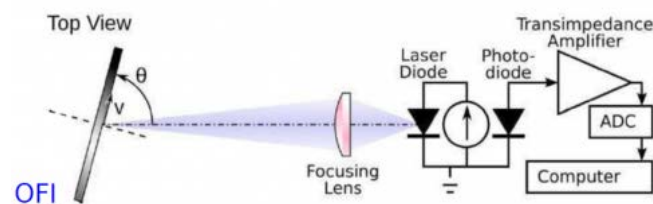


Figure 1. Optical Feedback Interferometry Scheme [15].

For Optical Feedback Interferometry technique, lasers diodes with a built-in package photodiode are used, the OFI signal can be easily acquired from the photodiode's current after an instrumentation and amplification stage.

1.2 Optical Feedback Interferometry in Fluidics Sensing

The optical feedback phenomenon applied to the frame of the flow measurement could also be called optical feedback flowmetry. In this context, the power of the OFI signal is proportional to the amount of light re-injected into the laser cavity once backscattered by the particles contained in the fluid that traverse the laser beam.

In this context, back-scattering produced by particles flowing is related to the power density of illumination, since generally the calculation of the electric and magnetic fields inside and outside a spherical object is either how much light is scattered, the total optical cross section, or where it goes. These are features according the Mie Theory [2], [16]. The “sensing volume” in this case is defined as the volume where the scatterers are generating measurable contributions to the OFI signal [3].

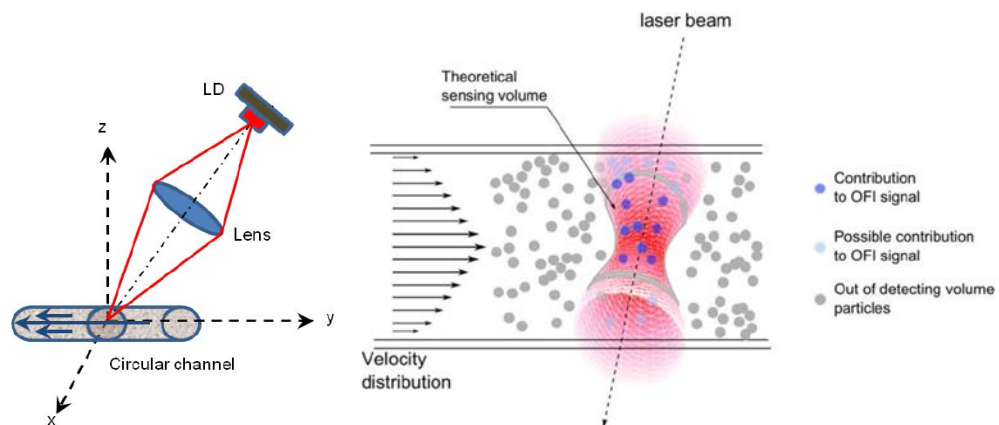


Figure 2. Schematic of OFI applied to fluid flow profile measurement [1], [17].

The main idea using the OFI technique to the fluidic systems is the possibility to determine the flow features studying the power spectrum of the light scattered by some particles contained into the fluid, this means that we will encounter several issues not present from scattering into solid targets, the most noticeable of these are:

- The light beam traverse different materials, which has different refractive indexes;
- Each particle inside the fluid move in a different direction according the other particles (little turbulence added);
- The scattering regime is volumetric (3 dimensional) instead of being over a surface (2 dimensional);
- One single photon could be scattered, so eventually it could be scattered by more than one single particle;
- Due to the micro-metric scale, the particle size could reach a comparable size with the laser wavelength.

These points affect the OFI signal, consequently, an analysis to deduce the flow parameters is required. These are going to be afforded after understanding the scattering regimes.

1.3 The Scattering Regimes

When targeting a flowing fluid, the particle concentration of it is an important element that affects the behavior since the particles inside the fluid are the responsible of the Doppler shift of light. As it was mentioned in the previous section, there could be characteristics associated between each particle such as direction, speed, distance, etc. [18].

When the particle concentration is low enough in a way that there are no adjacent particles and they are distanced each other, a single or independent scattering occur. In this case each photon is scattered by only one translating particle at the time, meaning that each particle own a unique velocity considered as an elementary scattering unit in a macroscopic medium composed of discrete particles randomly located [3].

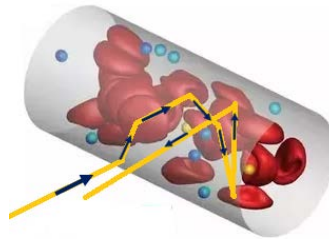


Figure 3. Light scattering with particles embedded in a fluid. The light (yellow) is scattered by more than one particle [19].

Otherwise, if the concentration contains a high density of particles, photons may be scattered several times by different particles before being re-injected in the laser cavity. This is known as the multiple scattering regime, and the OFI output power signal resulted due to this condition corresponds to a distribution of Doppler shifts, this means that the spectrum shape is affected by the multiple Doppler shifts returned in the laser cavity [19].

This internship work was focused in the biomedical applications using the OFI sensing technique, according the blood flow. However, there were used milk dilutions instead of blood to perform the experiments since the milk is an interesting fluid to be employed as an optical phantom for blood [16].

1.4 Flowmetry using OFI

1.4.1 OFI for Flowmetry.

The measurements using the OFI-based technique are analyzed using the Doppler Spectrum, regarding the velocity of the flowing particles. The Doppler spectrum is generated from the contributed feedback due to the particles contained in the fluid and its morphology is strongly related to the velocity distribution inside the sensing volume [17]. Thus, the amount of particles in the sensing volume is an important factor in the spectrum distribution.

A particle detection using the OFI sensor is made by focusing the laser sharply at the center of the microchannel where the particles are passing through with a laminar flow well

established. The dynamics of backscattering is ruled by the scattering cross-section of the particles against the power density of illumination [20].

Since the main focusing is according with the multiple scattering regime, the high concentration in the fluid will cause a significant change in the signal power spectrum of the OFI sensor. It has been demonstrated that the modulation of the laser output power (P_f) due to optical feedback in this case could be considered as the sum of all the scattered power contributions from each particle in the sensing volume [5].

$$P_f(t) = P_0 \left[1 + \sum_i m_i \cos(2\pi f_{D,i} t) \right]$$

Where P_0 is the initial power, f_D is the Doppler frequency shift due to the target speed, m is a constant that defines the feedback strength and t is the time.

1.4.2 OFI Flowmetry Methods.

A flowing particle produces the back-scattered wave that interferes in the laser cavity, and that carries the information about its speed [2]. The Doppler frequency shift (f_D) that affects the returning wave is given by

$$f_D = \frac{2nV_T \sin(\theta)}{\lambda}$$

Where n is the refractive index of the fluid, V_T is the speed of the target, θ is the angle between the laser beam and the normal to the flow direction, and λ is the laser wavelength. However, in most of the liquids, the high particle concentration will produce the measurement of a Doppler shifts distribution.

Thereby, depending the type of morphology of the encounter power spectrum, different methods has been proposed to extract the Doppler frequency from the power spectrum correspondent to the average speed of the fluid at the sensing volume.

Based in the article written by R. Bonner and R. Nossal in 1980 [21], where they define a model for blood perfusion measurement, the result of the analytic relationship that exist between the mean number of scattering events for a single photon, the particle size and the mean of the particle speed is used. This is defined as the spectrum moment as:

$$\langle \omega^m \rangle = \int_{-\infty}^{+\infty} |\omega|^m S(\omega) d\omega$$

The first moment of the spectrum gives information both on the average speed and the concentration of particles inside the flow. After de Mul et Al [8], studied more detailed this relationship, and develop a method that also relate the zero order moment and the second order moment with the flow speed, called as the weighted moment estimation of the power spectrum. In other words, the weighted moment is the ratio of the first order moment by the zero order moment.

$$\bar{f} = \frac{M_1}{M_0} = \frac{\int_{f_{min}}^{f_{max}} f PSD(f) df}{\int_{f_{min}}^{f_{max}} PSD(f) df}$$

Where \bar{f} is the average Doppler frequency, M_1 is the first order moment, M_0 is the zeroth order moment, f is the frequency, PSD is the power spectral density and f_{min} and f_{max} define the spectral frequency range where the signal is considered.

The moment evaluation seems to be a good way to achieve information about flow parameters, and in order to reduce the noise contribution at lower and high frequencies respect to the Doppler contributions, the moments are defined as the sum over the frequency range. This range is chosen looking at the spectra in order to optimize the moment evaluation and its dependent of the experimental configuration [19].

1.5 OFI for Flow Imaging

The possibility to use the OFI sensing scheme to build 2D Doppler images was demonstrated, however the scanning time was considerably high. Conventionally, the flow detection was done using a displacement system along the area of interest, taking measurements point by point in two dimensions. Additionally, for each position, several positions are acquired, resulting in long dead times, consequently an important trade-off between acquisition time and image quality exists.

The image built is done by exploiting the moment calculation, since the first order weighted raw moment (M_1) is proportional to both the speed and the amount of particles which contribute to the Doppler frequency shifts [7], we could use it to build the pattern of the physical flow path by performing additional signal processing.

As it was mentioned before, the setup configuration is linked to the moment optimization. For optimal conditions, we should be properly focused in the target and we should count with a high speed response 2D displacement system together with a data acquisition system with good sampling frequency, resolution and accuracy.

The classic flowcytometry requires the manipulation of the fluid content, previous to the data acquisition to obtain its parameters. OFI sensors focused in flow imaging and characterization tend to a direction where the blood perfusion, diagnostic and particle characterization could be done using a non-invasiveness sensor, which make their improvement and development very attractive.

CHAPTER 2

OFI FLOW DETECTION

Using one optical scheme, we are looking to perform the flow monitoring, this is based in the use of double lens for sharper focusing and tight sensing volume extension. The automatic focus over the microfluidic channel was done by combining two signal processing methods on the multiple scattering regime.

2.1 Experimental Set-Up

2.1.1 Microfluidic Channel.

For the auto detection of the micrometric fluidic channel we decided to use a single duct made with polydimethylsiloxane (PDMS), which is an organic polymer with low cost and manufacturing simplicity. A good advantage of this material is that it has the property of being hydrophobic, thus, most of fluids will not deform the channel or could leak from it.

This microfluidic channel has a circular shape of $320\mu\text{m}$ of diameter with a length of approximately 230 mm, in this way the maximum-to-average velocity ratio (k) is equal to 2. Its construction was already done by the LAAS researchers team. It was done using an optical fiber inside the PDMS mold.

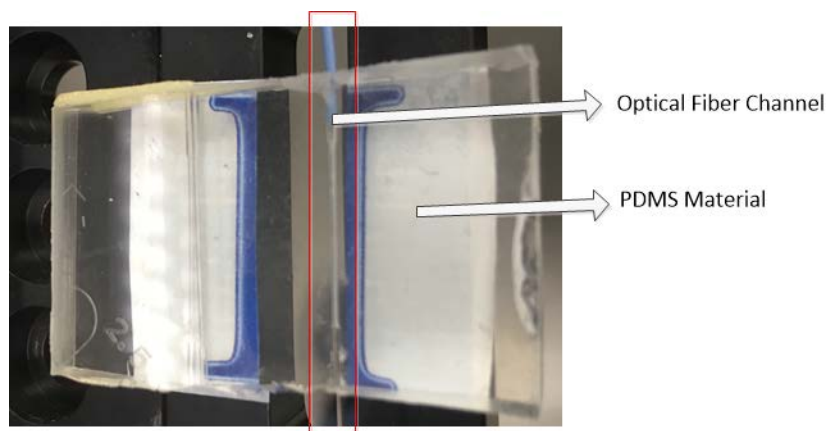


Figure 4. PDMS circular micrometric fluidic channel.

The hydrodynamic characterization of this PDMS circular duct is important to obtain for each volumetric flow provided into it. The average speed inside this channel corresponds to Q/A (where Q is the volumetric flow rate and A is the duct area), and it is a key parameter to analyze the Doppler frequency correspondent to the speed of the flow when the laser is focused over the channel.

$$A_{channel} = \pi r^2 = \pi(160e^{-6})^2 = 8.0425e^{-8} [m^2]$$

Additionally, the PDMS material has low reflectivity which is an advantage during the channel recognition, since the flow is likeable to have much more power compared to the material of the microfluidic channel.

2.1.2 Electronic System Scheme.

The hardware configuration for the flowmetry system is composed by several arrangements which allows the signal measurement and post processing.

First of all, to obtain the OFI signal, we used a Fabry-Pérot laser diode Thorlabs L785P090 (wavelength of $\lambda = 785$ nm, 90 mW of optical power) with a built-in package monitoring photodiode in charge to monitor the output power. Together with the laser, a custom made circuit that comprises a laser driver current source and a transimpedance amplifier with a gain of $135.64 dB_{V/A}$ and a bandwidth of 3 MHz approximately, provide the signal which was measured.

The OFI signal was captured using a data acquisition board (DAQ Board) National Instruments USB-6361, with 16 bits of resolution and a sampling frequency up to 2 MHz, however due that the maximum volumetric frequency used is $100 \mu L/min$, the sampling frequency was fixed to 100 KHz.

The optical configuration of this system is based using the combination of a collimating and a focusing lens for the OFI sensing scheme. By using this configuration, we can improve the signal to noise ratio (SNR) with the increment of power density in the micrometric volume and improving the back-scattering light collection as the focusing lens is closer to the target.

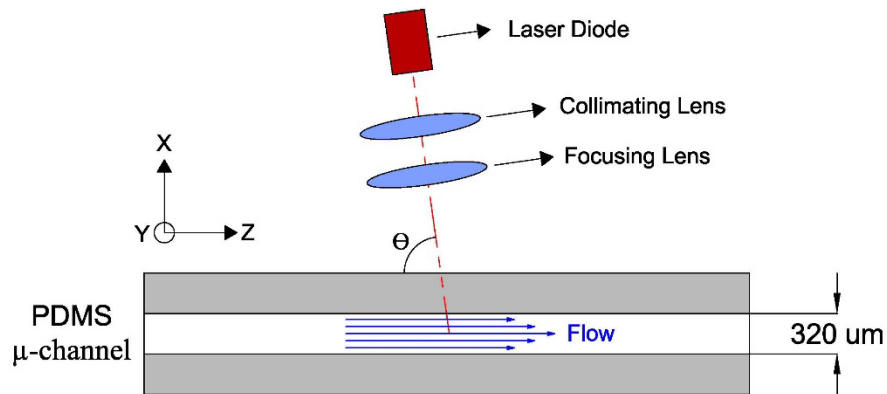


Figure 5. PDMS microfluidic channel, with laser scheme using two lenses.

The optical arrangement was done using a collimating lens Thorlabs C660TME-C and a focusing lens Thorlabs AL2520M-B, with a focal length of 20 mm. The optical angle Θ was tilted by 82° with respect to the flow direction, this angle has been proved in previous works [3], [22], [23] to be suitable for flow measurements.

2.1.3 Hydrodynamic Supply System.

One important requirement in flowmetrics is to ensure the supply of a laminar regime of the flow, to ensure this condition we used a microfluidic flow control system Fluigent MFCS-EZ with a flow monitoring platform Fluigent FRP. This system allows us to control the supply flow and monitor it via the Fluigent Flow-Rate-Platform in the PC where we can control the pressure in mBar of the system and measure it concordance in volumetric flow ($\mu\text{L}/\text{min}$).

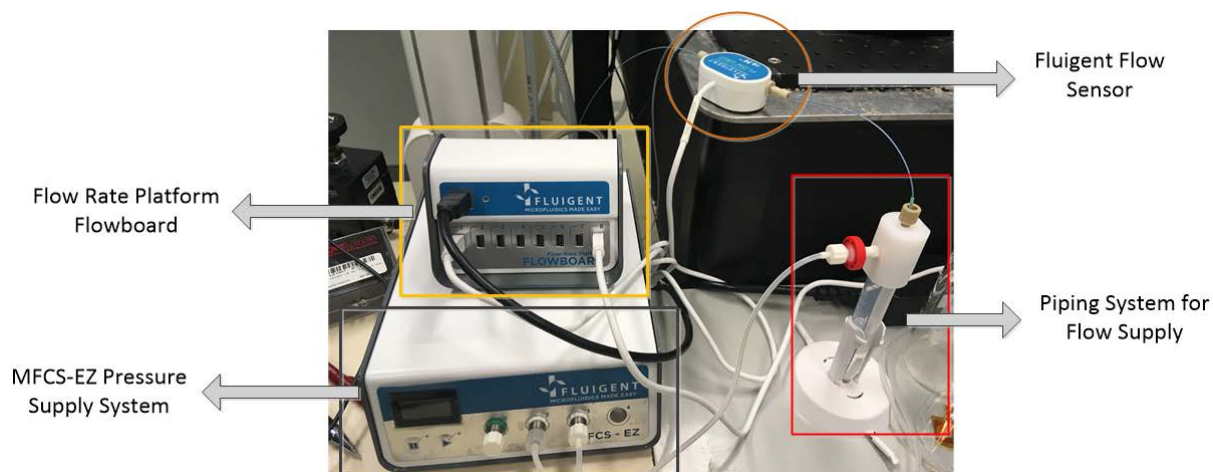


Figure 6. Hydrodynamic Supply System.

The Figure 6 illustrate the different components of the hydrodynamic system, this basically require a pneumatic supply via the MFCS-EZ device, which transform this air flow into liquid flow using a piping system, where the air is injected into a tube with the dilution where the pressure effect make the liquid insert in the micro piping system.

The dilution was done with bovine full cream milk, as it was mentioned, milk is a good phantom of blood. The size of the milk fat globules is from 1 μm to 10 μm which is similar to red blood cells, and their concentration ensures the multiple scattering regime. After the insertion of the dilution into the micro piping system a flowing sensor is located to monitor it volumetric flow.

A great advantage to use this platform is that we count with the software “Microfluidic Automation Tool” where additionally we can establish the set point of the volumetric flow in $\mu\text{L}/\text{min}$ and the pressure system will automatically adjust, allowing us to study directly the power spectrum change by the influence of the speed of particles in the channel.

2.1.4 Displacement System.

The measurements are taken using a motorized displacement system which consists in 3 linear stage motors Zaber Tech T-LSM050A, with a minimum micro-step resolution of $0.0476\ \mu\text{m}$ and a maximum speed of $6\ \text{mm/s}$. These characteristics permit the measurements in micro scale necessary for the detection of flow in the microfluidic chip.

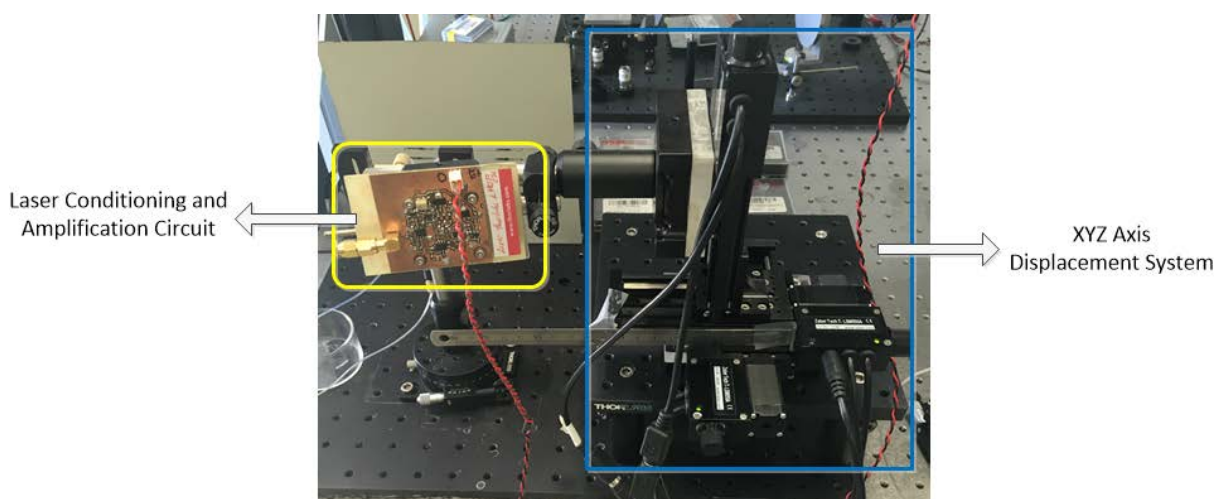


Figure 7. 3 Axis (XYZ) Displacement System Configuration.

The disposition of these motors are in a way that we form a XYZ axis directions displacement systems, and in this way we can ensure the proper focus point in the center of the channel, where the sensing region will fit the profile of a Newtonian fluid.

The small resolution of this system allow to displace with more accuracy over the area of interest, so by this way we ensure that the displacement system has the capabilities to focus over the microfluidic channel. And the three freedom degrees allow us to put the target in different positions or take the measure changing direction easily.

2.2 Acquisition Logic and Continuous Scanning Improvement

The detection of the microfluidic channel is the first and most important step to fulfill in flowmetry, since a proper focusing into the channel means the best signal acquired to process and study later. This procedure is difficult to achieve since the shape of the channel, the geometry of it and the reflectivity property of the target could lead to different type of measurements.

In our set-up, previous works did the detection and focus in the channel manually, meaning that the three axis displacement system should be commended in order to move step by step and controlling the step of movement of it, until it reaches the best point which corresponds to the center of the channel based on the measurement of the data acquisition board taken simultaneously.

One of the most important facts and improvements during our measurements is the continuous scanning technique. Kliese et al [24] used this to analyze the concentration of the fluid in a serpentine chip. Based in that proposition, during this work, one axis (X or Z) is moving along it direction while the data acquisition board is taking the signal at the same time. It is important to consider that this may add several undesired components to our measured signal which were suppressed in the signal processing.

The algorithm of autofocusing in the channel starts with the adjust procedure of the Z axis, which is aligned in parallel direction to the micro channel, this axis will be fixed in the middle of the range of operation of the Zaber Tech motor, which means in 25 mm of the 50 mm total range, in order to ensure that we are going to pass through the channel. A good position of the microfluidic chip is highly required to accomplish the channel detection.

Then continues the procedure of the Y axis, which is the direction to control the proximity to the microfluidic channel. This will perform 10 steps of 5 mm each one according

the proximity of the chip. The idea is to find the best point that ensures a good output power measurement. This suggest that we should be careful in the location of the microfluidic chip in order to avoid collisions between the laser and the fluidic channel.

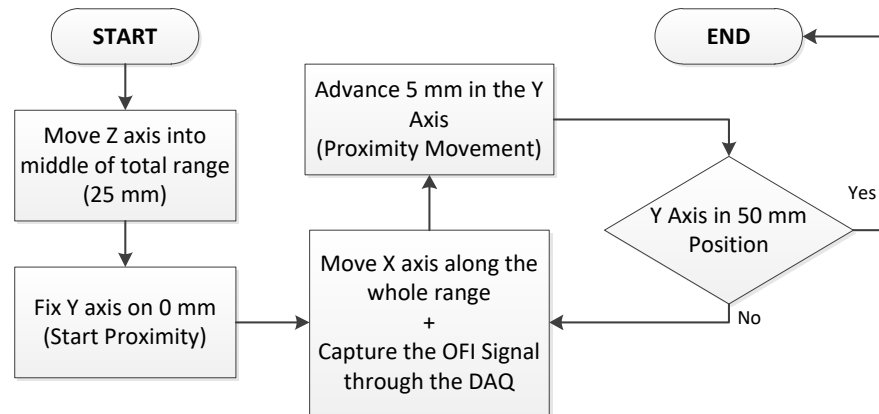


Figure 8. Algorithm Logic Flow Diagram.

However, the Y axis and X axis work are linked, since as long as the Y axis changes the position in proximity, the X axis will move over the whole range of the motor while the data acquisition board will take the measurement simultaneously. In other words, for each proximity step, a whole measure of the piece where the channel is located, is taken. All this described procedure is showed and described in the Figure 8 which is the flow diagram of the algorithm and logic.

2.3 Signal Processing and Microchannel Algorithm Recognition

The signal processing is done after the acquisition of all the measurements, and is based in two directives to estimate the center of the channel.

- The time domain signal acquired for each proximity position is analyzed in terms of fluctuation, the main idea is to identify where are located the possible points of flowing fluid in the voltage signal due to the abrupt variations given.

- The power spectral analysis is done similarly to each proximity signal, through the computation of the zeroth order moment which is a universal approach to evaluate the spectral energy of the signal.

The fluctuation in time domain detection in addition to the zeroth order moment might cover the concerned features required to identify the position of the channel and the center of it.

Using the fluctuation analysis, we intend to find where are the structural corners of the channel, since the sudden change of reflectivity contribution would cause a drastic fluctuation when the laser is passing through it.

The zeroth order moment computation of the signal, as it was mentioned, impart us the power energy concentrated in each position, so, this process might allow us to detect the higher concentration of particles in the middle of the channel.

Both results are combined in an algorithm which consists in three stages:

- The structure borders of the channel and the maximum concentration of the flow should be in concordance with the same physical distance, since we can obtain the physical displacement using the time of the signal using the speed of the motor, the coordinate of the channel could be obtained.
- For each proximity measure, the same criterion is used, and there are determined the three measures where the concentration of energy and fluctuations were higher during the whole proximity range.
- Based on the three previous results, an interpolation criterion is used to calculate the best Y position, then if the structure borders are in accordance with the high concentration, the higher peak of the zeroth moment is selected as the center of the channel in X axis, and the Z axis will remain as the middle of the whole trail.

This process is explained in detail in the Figure 9, where a flow diagram of the detection of the best focus coordinates process is presented. The algorithm is performed after the data acquisition process, and the result of it is the three best coordinates for the motor displacement system to focus in the middle of the micro channel.

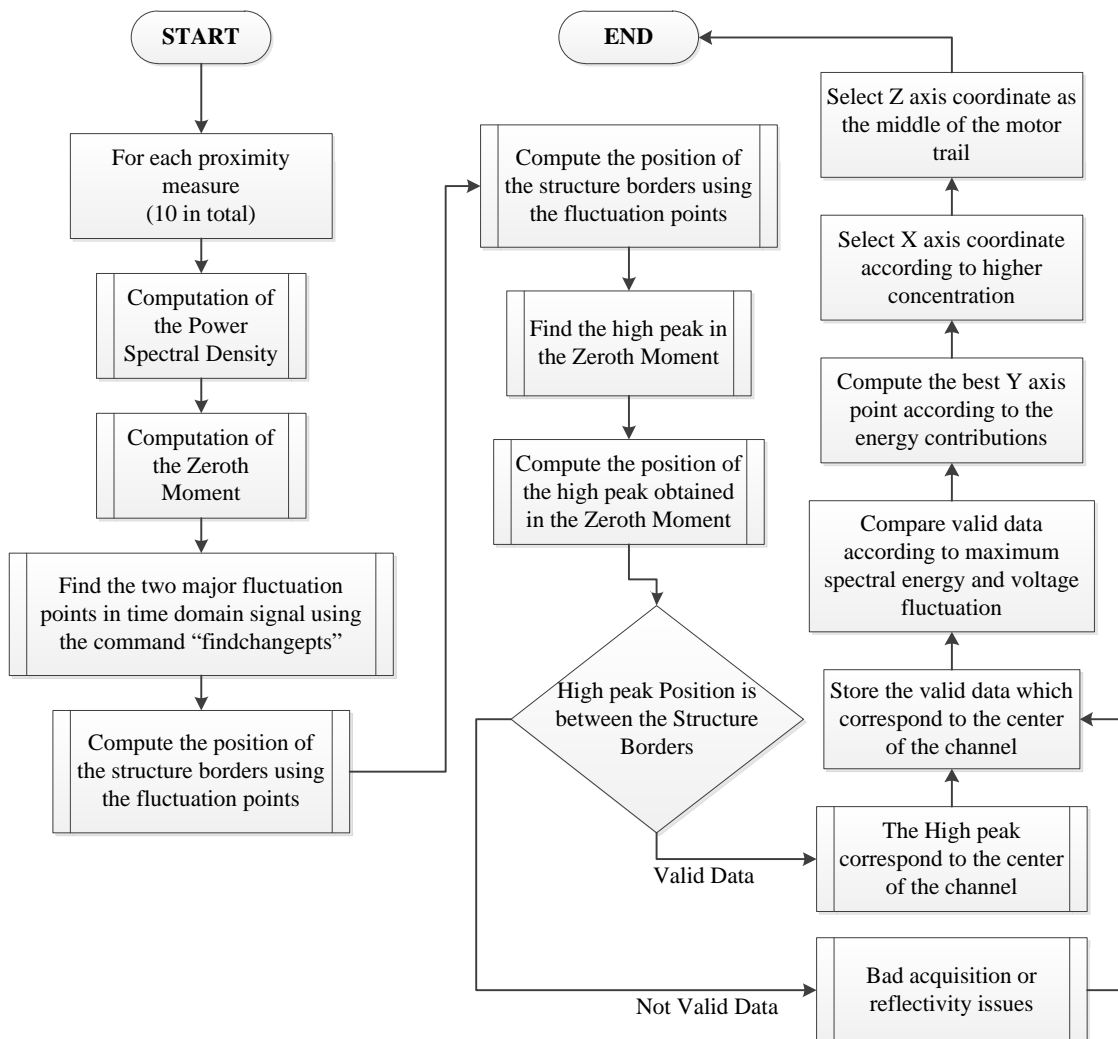


Figure 9. Signal Processing Algorithm Flow Diagram.

Data acquisition and Signal processing were done in MATLAB®, where we took advantage of the “Data Acquisition Toolbox” to generate and establish the interface with the National Instrument DAQ properly, and the “Zaber Device Control Toolbox” to command the displacement system. Additionally, a program which contains the algorithm scripts and a

graphic user interface (GUI) was developed in the App Designer to obtain a more intuitive interface.

The graphical interface designed contain the sections necessary to stablish the connection with the data acquisition board and the stepper displacement system which are the first steps that should be considered before any action. The graphic interface contains only the manual mode to control the displacement system, this was intended to enter the detected coordinates after the channel recognition script. There is also the section concerned the imaging system which is going to be explained forward.

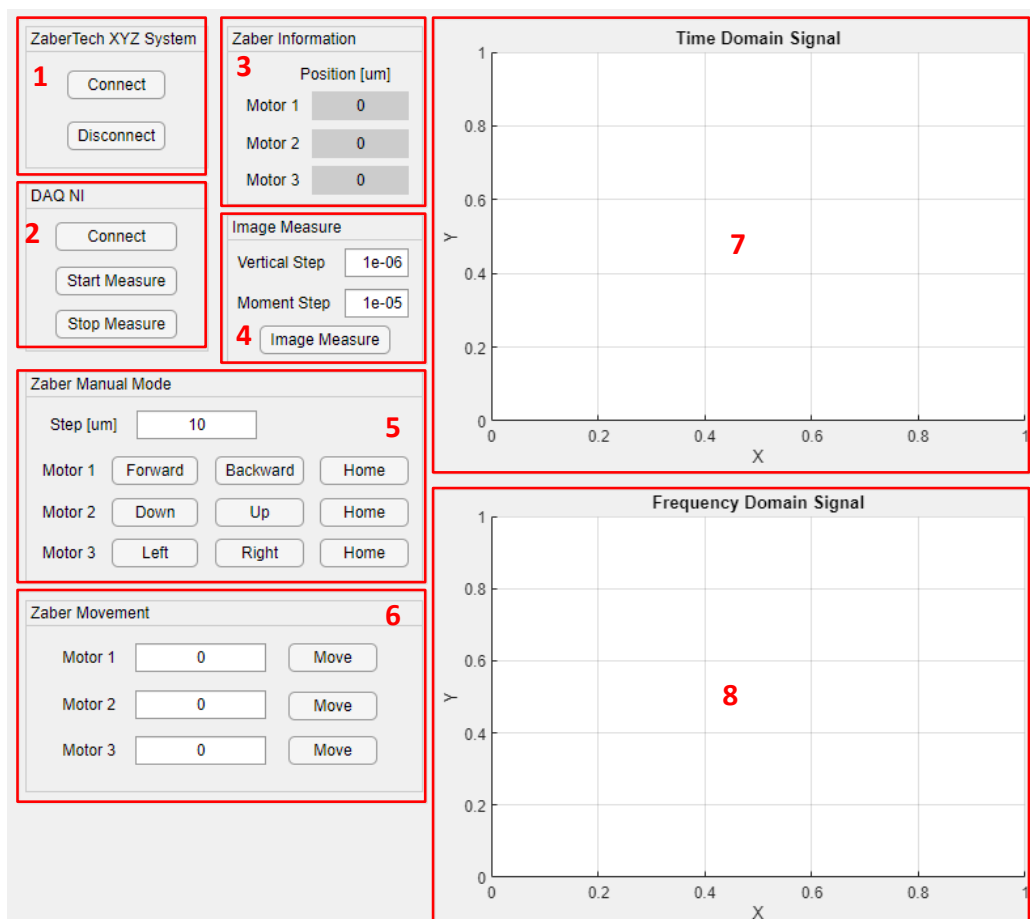


Figure 10. Graphic User Interface Created to perform data Acquisition.

Table 1. Description of the graphic interface developed.

Number	Function	Description
1	Zaber Tech Connection	This section calls the Toolkit in charge to establish the connection and send the commands to the Zaber Tech micro steppers
2	DAQ Connection	The Data Acquisition Toolkit is called during this section when we can establish the connection with the DAQ board and after start the measurement to display in the two different charts
3	Information of Zaber Tech System	This section will contain the information about the coordinates of the displacement system all the time.
4	Imaging Parameters and Acquisition	The imaging system requires the parameters of vertical step and moment step to compute the segmentation of the signal (this is explained in the imaging section) and we can initialize the image acquisition and construction
5	Manual control in "teach pendant" style	The "teach pendant" controls allow the user to move the displacement system step by step and change the step parameter.
6	Manual control with coordinates	This section allows the movement of the displacement system by specifying the exact coordinate in μm that we want to reach

7	Time domain signal chart / Image displaying	This chart will display continuously the time domain signal in manual mode (with 2MHz of sampling frequency and 4096 samples of signal), and the imaging results in imaging mode
8	Power spectral density chart	This chart will display the power spectral density of the signal displayed in time domain, the frequency range will be 1MHz.

The Table 1 details the sections that we can encounter in the graphic interface displayed in Figure 10, which contains the manual control and monitoring of the system in addition the imaging parameters.

2.4 Results

For the channel auto detection, we have tried different milk dilutions at a concentration by mass in water, but from previous works and from the manual detection of the channel, we have tested 1%, 2%, 5% and 10% w/w concentrations and the conclusion is the same than in previous works, where the concentration is higher we will have more scatters contribution, meaning that our signal will be better, thus, we proceeded only with the concentration of 10% w/w.

For the volumetric flow, we kept a constant flow rate of 50 $\mu\text{L}/\text{min}$, which ensures a high power measure of the OFI signal, we should take into account that not all the channel sizes will support the same maximum flow, for this case the microchannel support 200 $\mu\text{L}/\text{min}$ as maximum.

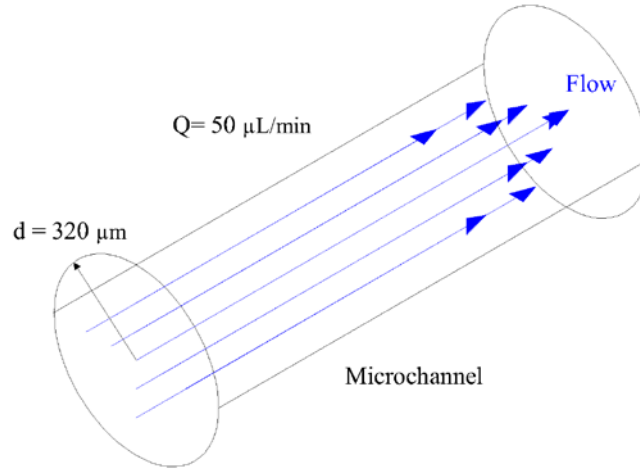


Figure 11. Microchannel dimension and volumetric flow rate.

From the Figure 11 we can obtain the speed of the fluid which is traveling through the microfluidic channel, this is important to obtain the Doppler frequency related to the flow, and also the Doppler frequency related to the movement of the displacement system.

$$v_{flow} = \frac{Q}{A} = \frac{50 \mu\text{L}/\text{min}}{\pi * (320 \mu\text{m})^2} = \frac{8.33e^{-10} \frac{\text{m}^3}{\text{seg}}}{\pi * (320e^{-6} \text{m})^2} = 0.00259 \frac{\text{m}}{\text{s}}$$

$$f_{D_{flow}} = \frac{2 \eta v_{flow} * \cos(\theta)}{\lambda} = \frac{2 (0.00259) * \cos(82^\circ)}{785e^{-9}} = 918.36 \text{ Hz}$$

The first experiment was performed using different speed rates of the displacement system as it is showed in the Figure 12. The objective was to see how much affect the measurement of the signal as long as we change the speed, one of the most important things is to notice the fluctuation due to the microchannel zone.

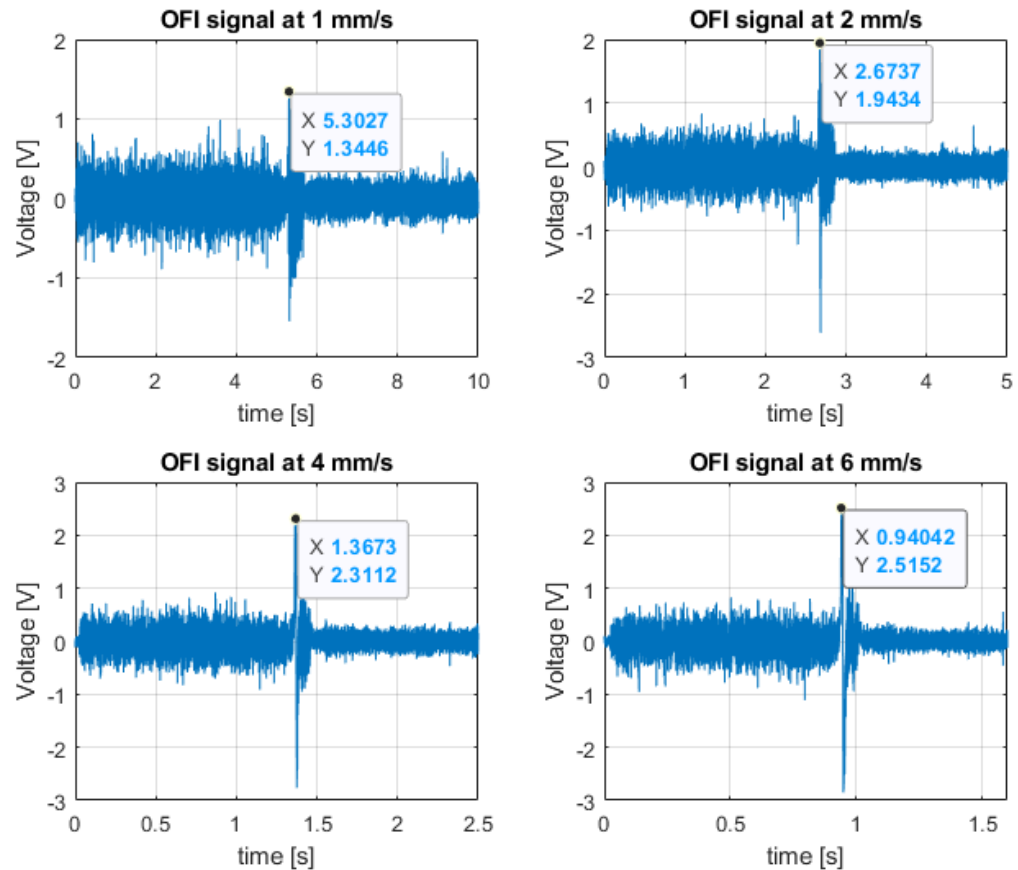


Figure 12. OFI signals fluctuations at different speed of the displacement system.

The most noticeable difference between changing the speeds in this case, is the signal level at the fluctuation point. As we can observe in the Figure 12.a with 1 mm/s of speed the signal level is changing noisily until the microchannel is reached, when this happens the signal has a small fluctuation up to 1.34 V. As long as we increment the speed to the maximum which is 6 mm/s, we experiment a bigger fluctuation after reaching this point. The increment is from 1.34V to 1.94V, 2.31V and 2.51V according to 2 mm/s, 4 mm/s and 6 mm/s respectively.

It was decided to work with the maximum speed that the displacement system can provide, since the contribution due to the reflectivity of external factors and the displacement speed do not have a heavy repercussion in the OFI signal, the speed of 6 mm/s may increase the time efficiency of the system.

$$f_{D_{zaber}} = \frac{2 \eta v_{zaber} * \cos(\theta)}{\lambda} = \frac{2 (6e^{-3}) * \cos(82^\circ)}{785e^{-9}} = 2.1275 \text{ KHz}$$

Since we have only low Doppler frequencies, even if we can use high sampling frequencies, it was decided to use 100 KHz which would cover the entire contributions given by the two major interest components. The frequency contribution due to the movement of the system for the PDMS do not affect dramatically to the detection of the more power concentration where the center of the channel is located.

By applying the algorithm to the channel with the fluid flowing at 50 $\mu\text{L}/\text{min}$ we have obtained several measurements for each proximity change, the more interesting to observe in this case is that as long as the laser gets far from the chip, the fluctuation is more noticeable, like it is the case of the Figure 13, where there are presented three different cases of proximity.

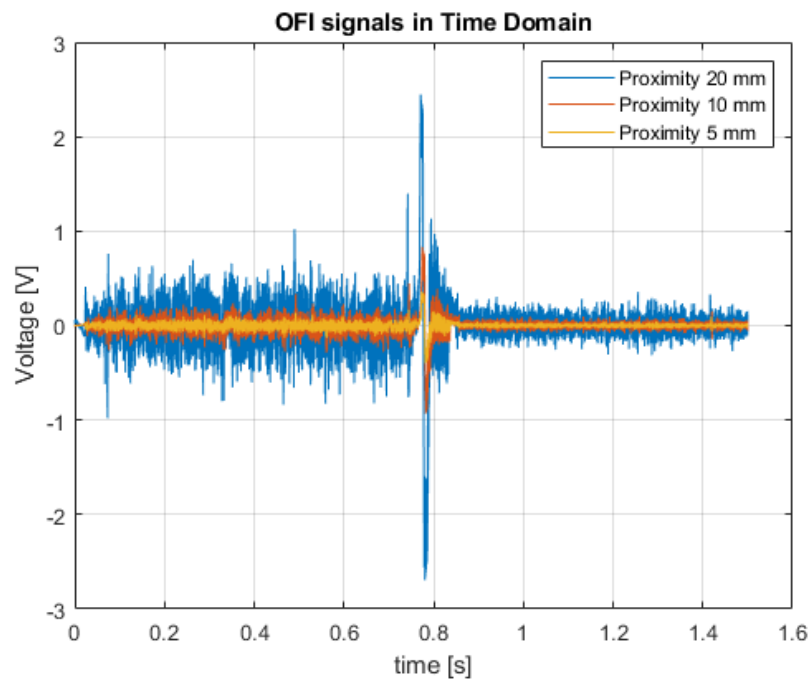


Figure 13. Different OFI signals in time domain.

As long as the laser finds far from the microfluidic chip the signal is lower in terms of voltage measured, but we can notice that the shape of fluctuation is quite similar, in Figure 13

when the laser is at 5 mm of its trail, the OFI captured signal is weaker than at the proximity of 10 mm and 20 mm, where it intensifies. One important difference in the signal is that the first section before the fluctuation has more noise than the second, this is due to a geometric disposition of the microfluidic channel which makes the OFI signal has a larger distance after the single channel.

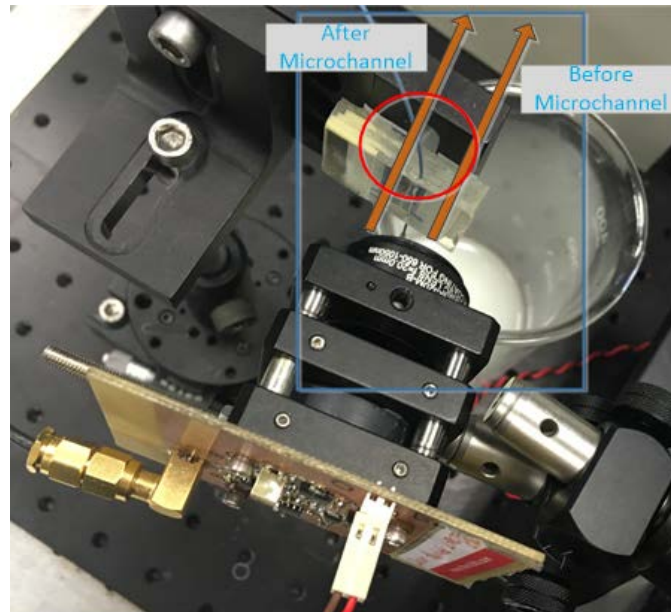


Figure 14. Laser Scanning direction, before and after microchannel (Upper View).

There is a spot behind after the microchannel, as it is showed in the Figure 14, and that contribute to the decrement of signal after the fluctuation point. Anyway, this does not affect the processing of the signal. The fluctuation of the OFI signal is one of the first verification processes, however the retrieved data works as a reassurance parameter to know if the maximum energy is concentrated within this region.

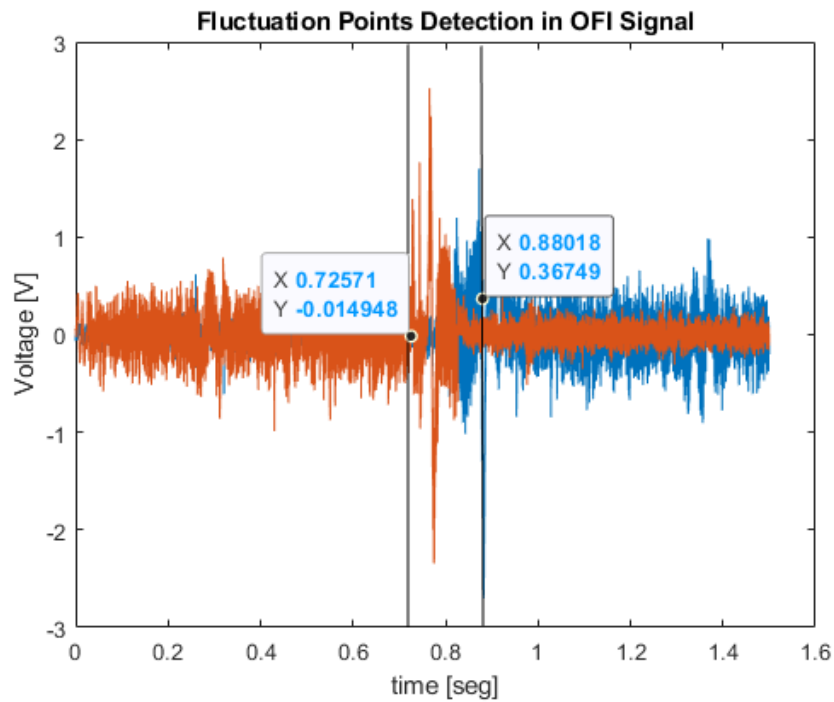


Figure 15. Fluctuation range detection of OFI signals in time domain.

The Figure 15 shows the interval where the two main fluctuations are encountered, and next to that we should analyze the power spectrum contribution given from the measured signals. The power spectral density of the signals is taken using the Welch method by the command “pwelch” in MATLAB®. In this method we can use a windowing method in order to overlap the samples and obtain a better spectrum since these are not periodical signals.

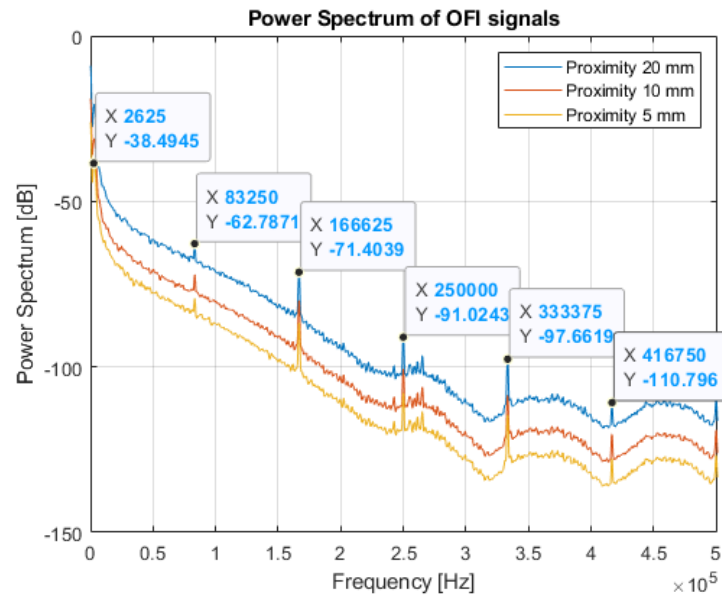


Figure 16. Power Spectrum of the OFI signals according to different proximities.

From the Figure 16 we can observe that the contribution in the power spectrum is similar as long we get near to the microfluidic channel. The interest frequency where the maximum energy contribution is located in the 2.625 KHz, which is quite different than the theoretical value but not differ dramatically. There are several harmonic contributions also, given by the movement of the displacement system and other external components.

Since the power spectrum only can provide us the shape of the power contribution at certain frequencies, we need to use the moment method to observe the power contribution at certain positions. To do that the moment method is applied to the power spectrum of different sections of the time domain signal. In other words, the time domain signal is analyzed in intervals to obtain an array of moments.

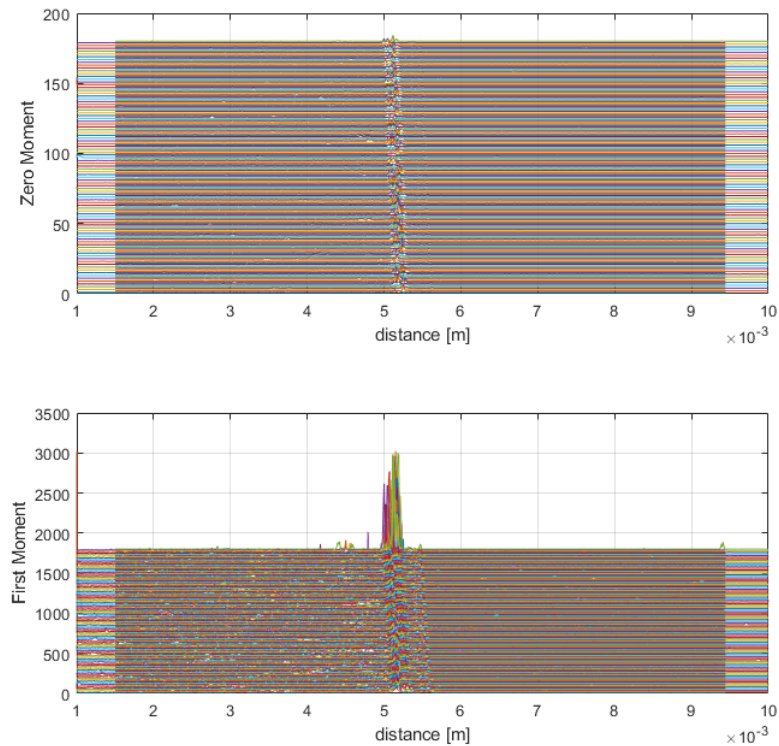


Figure 17. Zeroth and First Moments of the Power Spectral Signals.

One disadvantage of doing this is that the signal processing become heaviest since for each interval of the time domain signal require a computation of its power spectral density and after the moment method. In the Figure 17 we could verify the results of the zeroth and first order moments of the signal, the most important is to notice that the high concentration of energy is in the center of the channel, which ensure the proper detection.

Another important thing to notice is that the first moment provides a stronger contribution than the zeroth moment, but for the case of recognition of the center of the channel the zeroth order moment is enough. After the signal processing we obtained the coordinates of the center of the channel which after could be entered in the graphic interface. The algorithm during the tests with the physical arrangement result with the three coordinates for each axis (X: 29000, Y: 21000 and Z: 25000) which could be tested, it is important to remark that the Z coordinate is always fixed in the middle of the trail of the stepper.

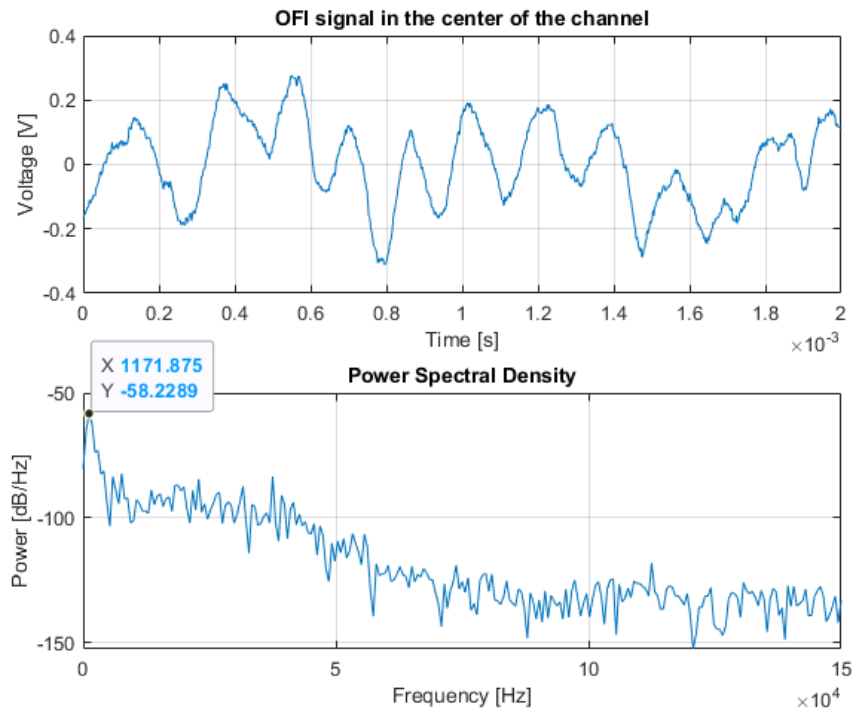


Figure 18. Measurement signal after entering the coordinates in the middle of the channel.

In the Figure 18 are displayed the result after entering this coordinates in the program, the time domain signal provide the fringes fluctuating due to the movement of the particles and the power spectral density displays the Doppler frequency at 1171 Hz approximately, which is not so different than the theoretical value of 918 Hz.

$$error_{f_D} = 253 \text{ Hz} \approx 21\%$$

Even changing the position of the X axis manually, do not improve so much the measure of the signal, so we can conclude that the algorithm worked as expected and this variation of the Doppler frequency is given by another factors such as reflectivity, temperature, pressure, etc.

CHAPTER 3

OFI IMAGING SYSTEMS FOR MICROMETRIC FLOW-PATTERNS

3.1 OFI Imaging System using a three axis displacement System

As it was mentioned in the introduction section, flowmetry at micro-scale had a great impulse in the bio-medical field, especially those concerned to the cell and tissue analysis where several parameters could be determined, inside this field we could find the bio-sensors, like is the case of advanced microscopes and cameras which recognize the flowing patterns for further disease study.

The constant tendency and need for compact and cheaper electronic systems for bio-applications is growing, so the development of this new sensor are essential. Using the OFI technology we intended to develop an imaging system capable to detect micro-scale flow patterns.

3.1.1 Experimental Set-Up.

For this purpose, we used the same equipment than in the flow detection mentioned in the previous section, with the unique change of the microfluidic chip. The Figure 19 show the diagram where it are displayed the disposition and arrangement of the components.

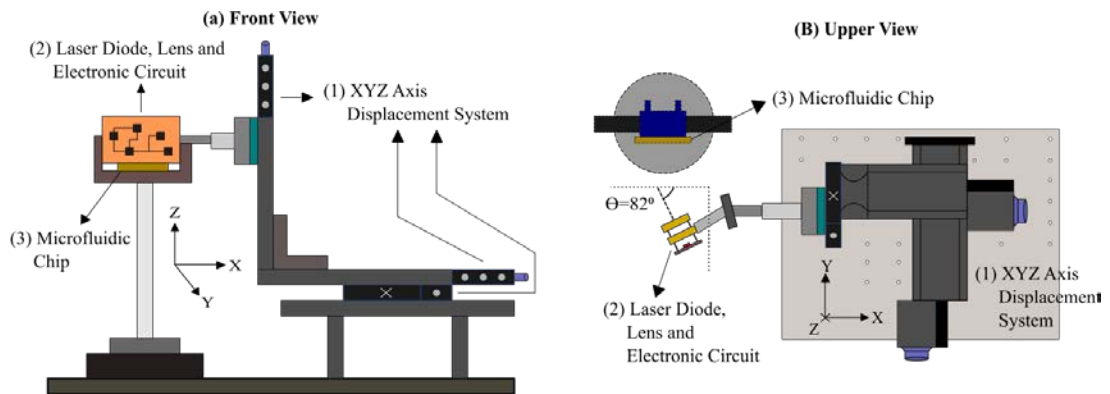


Figure 19. Experimental Configuration Diagram (a) Front view and (b) Upper view.

The hydrodynamic pumping system still and the data acquisition system still remains as previous as well. Now the microfluidic chip used contains a rectangular channel of $144 \times 48 \mu\text{m}$ (rectangular) in a serpentine shape, fabricated using a photo-lithographic process in a glass package.

By using this chip, we can study the micrometric flow pattern, since the serpentine form has changes from $150 \mu\text{m}$ where the curve section is greater, until $10 \mu\text{m}$ where there is the minimum spacing between channels. In order to detect the Doppler frequency shifts, the rasterization has been performed using an incidence angle of 82° in both Z axis (vertical) and the X axis (horizontal). Thus we were able to scan in horizontal and vertical evenly.

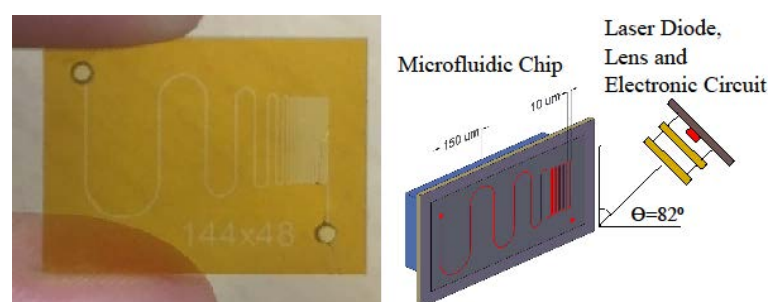


Figure 20. Photo-lithographic Microfluidic Chip (Serpentine form) and tilted angle.

The fluid used was a milk dilution as well, at a concentration by mass in water of 5% w/w, that was pumped at a volumetric flow rate of $10 \mu\text{L}/\text{min}$. Due to the small size of the

channel it is recommendable to use lower concentration than the previous case to prevent particles get stuck in the channel.

$$Area_{channel} = 6.9120 \text{ nm}^2$$

The rectangular microfluidic channel as compared to the cylindrical channel, this channel offers a lower region corresponding to the maximum speed and thus simplifies the lateral alignment of the laser beam. The speed had not surpassed the 10 $\mu\text{L}/\text{min}$ to avoid damage in the channel.

In addition, the microfluidic channel should be located inside a special support made to put the input and output pipe aligned with the channel, and integrate it with the hydrodynamic supply system. This support is showed in the Figure 21.

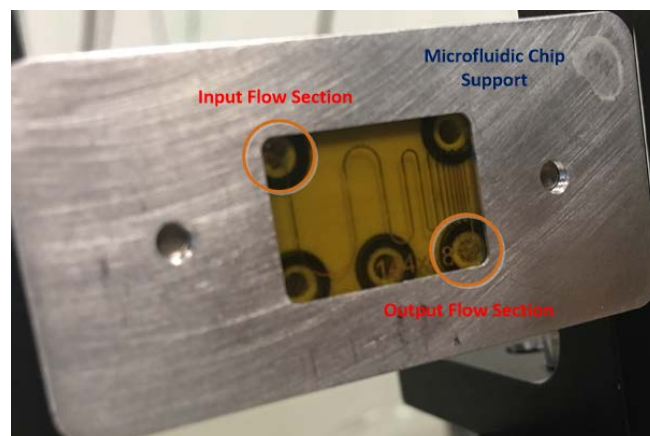


Figure 21. Microfluidic chip support for flow supplying.

3.1.2 Signal Processing and Continuous Scanning Integration.

One of the problems encountered in previous works in imaging using OFI is the time efficiency, because, so far the flow detection was done by moving the scanning system step by step in 2D over the area of interest. At each position, several samples were acquired for further process, resulting in long dead times and whereby the trade-off between acquisition time and image quality generally result in images that require hours of acquisition.

For this imaging system, it was proposed an OFI continuous scanning system, where one axis acquire the signal continuously while acquiring the OFI signal, as the second axis waits fixed until the first's translation terminates. With this approach, we considerably improve the acquisition time while keeping a high resolution.

The Y axis was used to focus over the target, which in this case is the serpentine microfluidic chip, while the X and Z axis (Horizontal and vertical respectively) were for 2D measurements. All the displacements were done with the maximum available speed of 6 mm/s of the micro stepper displacement system.

In the same way than the flow detection and monitoring case, the signal processing is based on the power spectral analysis of the OFI signal, through the computation of the first order moment of the Power Spectral Density (PSD). The Figure 22 presents the flowchart of the automation and signal processing for the image acquisition. However, before the whole process, we should consider that the resolution of the image is determined differently for each direction.

- In the fixed axis the step between each line of scanning determine the resolution. This is more limited to the displacement system, since as better step resolution it has, lower the step that we can select, meaning more resolution in one direction.
- In the continuous scanning axis, a segmentation of the temporal signal was done. Thus, the resolution is determined by the time of the segment which correspond to a certain distance/pixel.

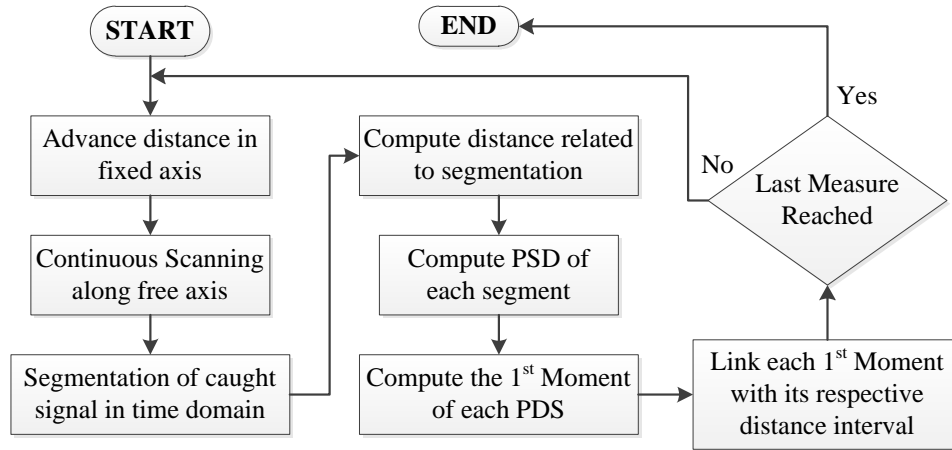


Figure 22. Flow Diagram correspondent to the measurements and signal processing.

The segmentation process is key in the image reconstruction from the acquired signal. Since the measurement is taking in time, we should consider that a certain selected time will correspond to a position in space, because both actions are executing simultaneously. Considering our case, we have a sampling frequency of 100 KHz according the acquisition system, and a movement speed of 6 mm/s concerning the displacement systems. Assuming a synchronization between both systems via the programming algorithms from MATLAB®, we can calculate the value of time and its correspondence to distance.

If we want to know how many samples we have to segment in an interval respectively to 1 μm , we can proceed to obtain it using the sampling frequency given.

$$f_s = 100 \text{ KHz and } v_{motor} = 6e^{-3} \frac{m}{s}$$

Taking in consideration that the speed of displacement is 6 mm/s, at 1 μm of distance we should have spent a time of $1.6667e^{-4}$ seconds in the travel. Each sample is taken at 10 μs from the given sampling frequency, so the total amount of samples in that time is 16.67 which is rounded to 17 samples per each μm .

The total amount of samples taken in the signal processing segmentation determine the resolution in the continuous axis acquisition direction, this may be treated as another trade-off, since as much samples we have, the signal processing will improve, but we will lose resolution. During the experiments with different segmentations it was decided that 10 μm which is translated into 167 samples is a good minimum value which remain high quality results in the image build.

The array of signals is acquired given the parameters of the moment step which corresponds to the OFI signal segmentation and the fixed step as inputs as it is showed in the Figure 10. From this parameter also depends how many time will require the system to catch all the necessary data to generate the image.

The algorithm is based in the segmentation of each OFI signal according to each step of the fixed axis, after that there is computed the PSD of each segment and after that the first moment of each PSD, the first moment since provide the proportionality of speed and amount of particles contributors to the Doppler shifts, is the key of the image flow-pattern location. More quality will require more segments, and as in any imaging system, there is a trade-off between the resolution and the acquisition and processing time.

3.1.3 Results.

To validate the proper operation of the imaging system, four different experiments were done, all of these are intended to demonstrate different characteristics and factor involved in the acquisition data.

A. Impact of reflectivity in continuous scanning and sensor resolution's limit.

The first experiment consists in computing the image of the full serpentine, first with vertical continuous scanning and then with horizontal. Since measurement and movement were

done at the same time, Doppler shift induced by the channel structure must be considered. It is important to determine its impact for both continuous scanning directions.

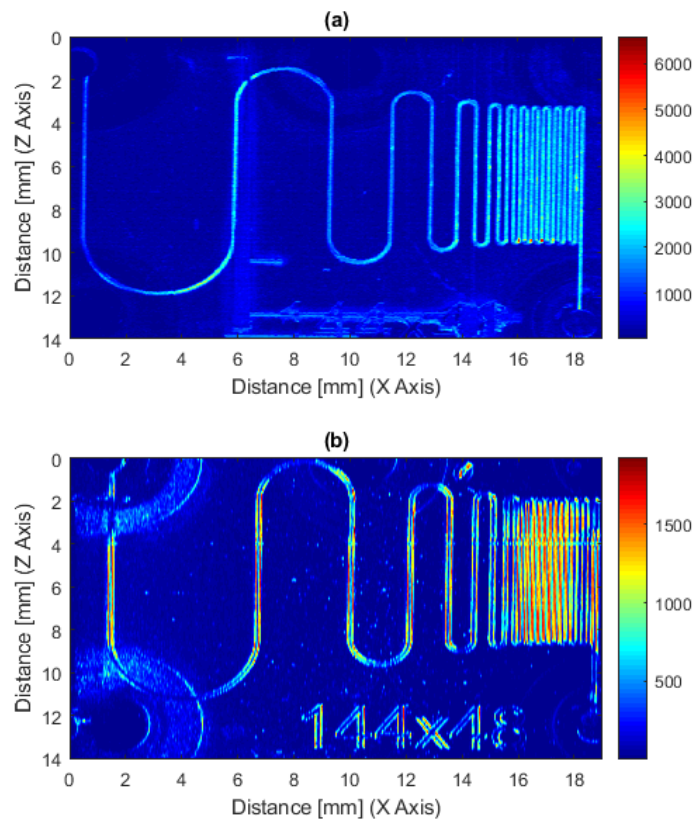


Figure 23. Image of all serpentine (a) Vertical scanning ($25 \mu\text{m}/\text{pixel} \times 10 \mu\text{m}/\text{pixel}$, total 608×1137 pixels Horizontal X Vertical), (b) Horizontal Scanning ($10 \mu\text{m}/\text{pixel} \times 50 \mu\text{m}/\text{pixel}$, total 800×214 pixels).

In the Figure 23 is displayed the results after performing the scanning changing the fixed axis and the continuous axis. The resolutions obtained are linked to the maximum allowable step of the sensor before experimenting distortion (blur) in the image, nevertheless, from it we can also notice the impact of each measurement direction.

- If continuous scanning is done in Z axis (vertical) (Figure 23.a), the laser displacement is done along flow direction. Therefore, reflectivities are only detected in the curves of the serpentine, and the flow pattern is easier to detect.

- Else, if it is done in X axis (horizontal) (Figure 23.b), measurements are mostly done in perpendicular direction of the flow. Therefore, the contribution of the reflectivity is more than the flow.

In conclusion, continuous scanning axis direction improves when it is done in the same direction (parallel vector) of the flow. Otherwise, when we are perpendicular to the flow direction, reflectivity on the channel walls could affect the Doppler image quality. All further measurements were done using the vertical continuous scanning since the horizontal scanning always would result in the measurement of the reflectivity walls of the microfluidic channel. Additionally, the measure of the serpentine also enables the determination of the maximum allowable step for the fixed axis before starting to get distortions in the image.

This limit is showed in the image in Figure 23.a, where the step is 25 μm . Using this we can observe the shape of the serpentine totally recognizable and the flow pattern clearly visible. Increasing the advance step more than this will produce distortion and decay in the quality.

B. Laminarity of the Flow.

The second experiment was done to determine the laminarity of the flow inside the serpentine. To do that, only one micro-metric channel inside it was measured by shifting it vertically distributed. Using a step of 1 μm in the fixed axis we took 200 vertical steps in total to measure 1 single channel.

After the measurement, the mean of all continuous measurements were done in order to obtain one single data for each vertical position, and by this way verifying where the flow concentration is located inside the channel.

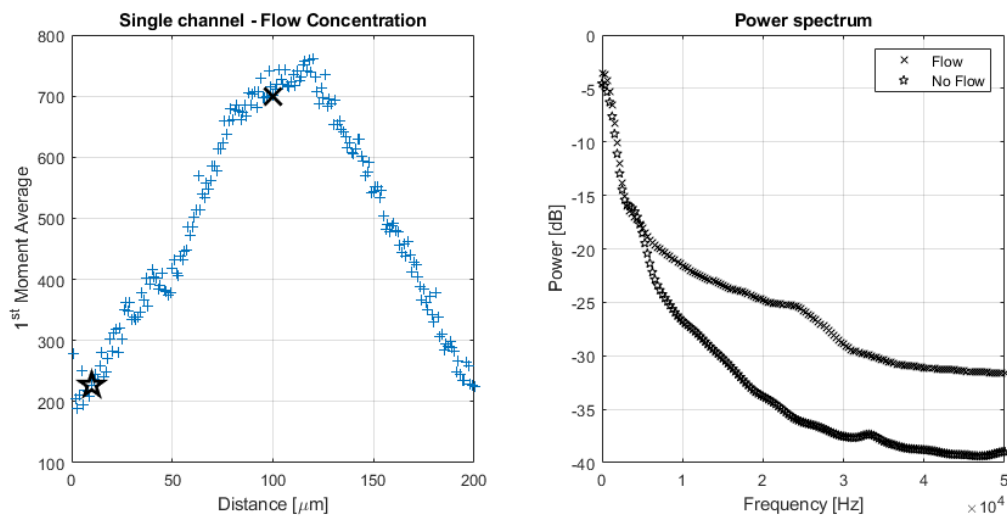


Figure 24. Single Channel Measurement over the Serpentine Piece, with 200 samples along the vertical axis (a) Flow concentration, (b) power spectrum of flow and no flow sections

The fluid has been proved to be laminar by analyzing the flow concentration and its major focusing in the middle of the channel according to the Hagen-Poiseuille profile for a Newtonian fluid (Figure 24.a). Also the contribution of the power in the spectrum is higher when there is flow than it is not (Figure 24.b).

C. Power contribution due to displacement.

The third experiment was intended to recognize the power contribution due to the displacement while the signal is being acquired. This is important since the signal processing is done using its power spectral analysis.

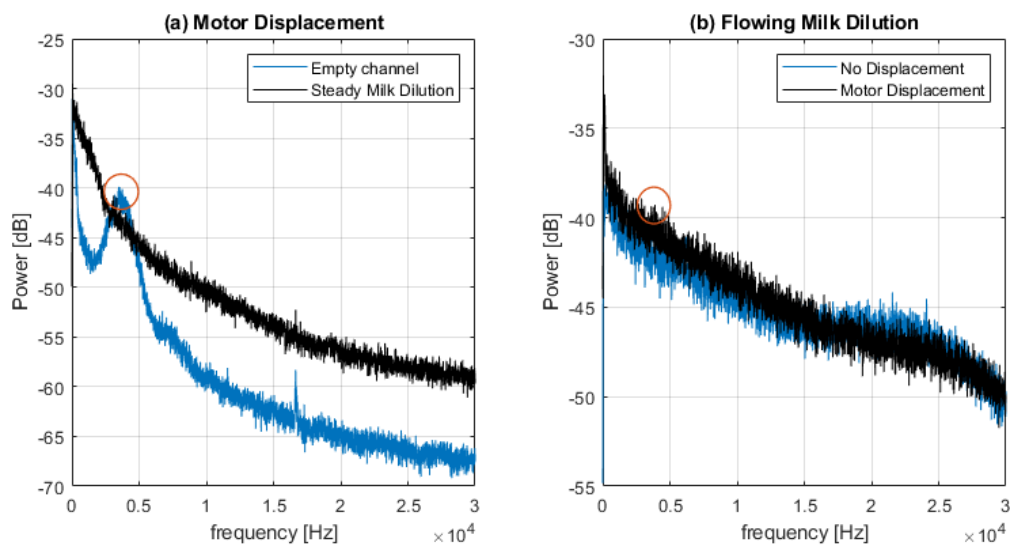


Figure 25. Power contributions with (a) motor displacement with empty and full of fluid channel, and (b) flowing fluid with displacement and without it.

Two different comparisons are showed, in the first the system was displacing through the empty channel and then with the milk dilution inside it, but without flow. And in the second we have the milk dilution flowing at 10 $\mu\text{L}/\text{min}$, and there were taken measurements for both with and without the movement due to the displacement system.

The power contribution due to the movement over the empty channel is clearly visible at approximately 3.5 KHz. (Figure 25.a), which approximately similar to the theoretical calculated value due to the motor displacement. However, when we add the milk dilution, different power contributions due to the dilution produces that the movement contribution do not be so noticeable, even if the power contribution remains, the shape is totally changed, we enter in the multiple scattering regime even without flow.

Finally this displacement contribution became hardly detectable when the milk dilution is flowing through the channel (Figure 25.b). The power contribution of the movement is difficult to detect due to other stronger contributions, which are related to the flowing flow and its properties. Even if the shapes are different when we add the displacement, it is not so

influential in the power spectrum, that is the reason why, when we are in the parallel direction of the flow, the motor displacement do not affect dramatically the signal processing.

D. OFI sensor acquisition time vs image quality.

The four experiment was done to determine the performance of the sensor, concerning acquisition time vs image quality, and also minimum detection distance. The measure was done across the section where is the minimum distance between channels, which is $10\ \mu\text{m}$. A vertical step of $1\ \mu\text{m}$ was used to verify a high quality definition image and the acquisition time. Three different results were obtained for this experiment (Figure 26).

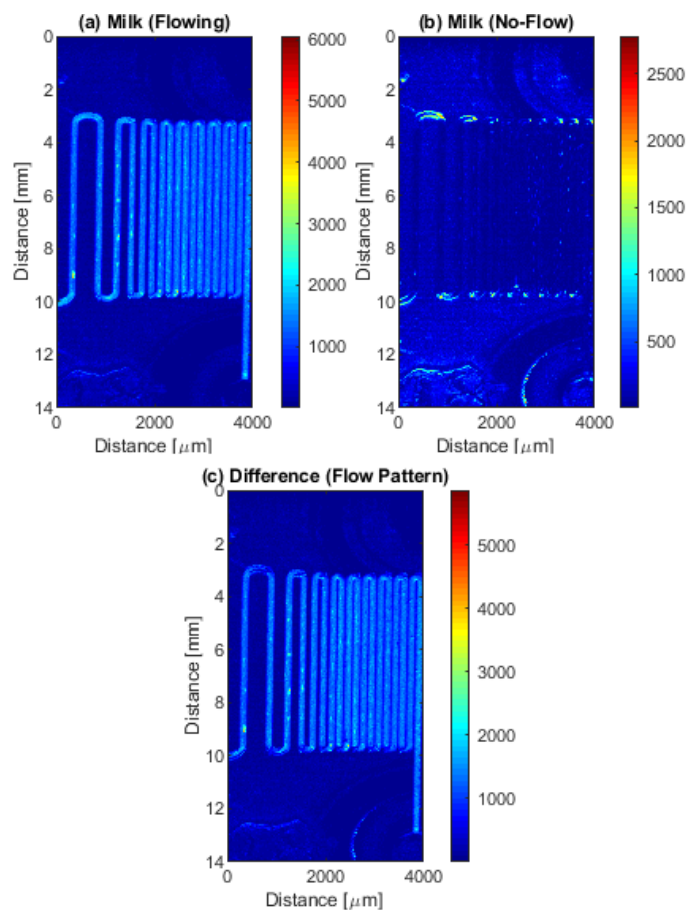


Figure 26. Section Image over the Serpentine ($1\ \mu\text{m}/\text{pixel} \times 10\ \mu\text{m}/\text{pixel}$) (4000×1097 pixels) (a) Milk dilution at $10\ \mu\text{L}/\text{min}$, (b) Steady milk (no Flow), (c)

Subtraction between (a) and (b) consonant to flow pattern.

- First is the scan when milk dilution is flowing at 10 $\mu\text{L}/\text{min}$, thus we can observe the concentration of the flow which basically determine the pattern of it.
- Second is the same scan but with no flow, thus we can notice the contribution of the reflectivity on the curves of the serpentine, which is the stronger parameter detected on this case.
- Third is the subtraction between both, which is consonant with the flow pattern since the reflectivity of the material has been removed in this operation.

Another important thing which is observed, is that the contribution due to the reflectivities in this case is much less than doing the horizontal scanning (Figure 26.b), so, even if the measurement taken is not subtracted the result is approximately the flow pattern.

We could verify the detection of the flow even at minimum distance between channels on the serpentine. Thus concluding that the 1 $\mu\text{m}/\text{pixel}$ resolution is being fulfilled and that flow concentration and pattern detection has been done as expected.

However, it is worth to remind that the horizontal resolution, linked to the fixed step advance, is limited by the physical capabilities of the displacement system, and that the vertical resolution, linked to the continuous scanning axis, is limited by the sampling frequency of the acquisition system.

The acquisition time for this image was 4 hours and 30 minutes, which is a back-off in the performance concerned in the time to achieve a very high resolution image. In spite of this, if we use bigger steps but not bigger than the limit, we can still obtain good quality images in much less time.

3.2 OFI Imaging System using Mirror Beam Steering

As we saw, in our previous implementation using the three dimensional displacement system approach, provided us good results, with high resolution and improving the scanning time. However, the compactness of this system requires a revision due to the size of the mechanical system.

This makes our system that remains in the experimental environment, since it requires a bulky displacement system which requires an important physical space, which in a practical or applied situation is no so suitable since the scanning system is moved with the whole OFI sensing system (optics and electronics).

Taking the advantage of the features of the OFI technology, it was proposed to use a prototype developed by the LAAS-OSE group, which implements an embedded displacement system, with the combination of the continuous scanning improvement.

This prototype has been developed by da Costa et al [7] to overcome these issues, using a new embedded OFI Doppler flow imaging system that uses a 2-axis beam-steering mirror mounted on a Micro-Electro-Mechanical System (MEMS), thus taking full advantage of the compactness offered by the OFI sensing scheme.

However, the MEMS based beam steering system entails into a more complex optical alignment, and in several cases the focusing is less efficient due to the absence of a movement focusing axis.

3.2.1 Experimental Set-Up.

The device is a handheld OFI sensor to monitor the skin blood perfusion. The new experimental setup as it was mentioned, replace the whole displacement system and the laser diode and keep the same microfluidic chip, fluid and hydrodynamic system.

The novelty of this solution starts with the inclusion of the Micro-Electro-Mechanical System (MEMS) which is a beam-steering mirror for the 2D scanning. The main objective of this development concerns the biomedical field, related to vascularization and microfluidic analysis, improving the innovation and non-invasiveness feature in this applications.

The entire handheld lasing system is composed by three main sub systems, each one of them have its own important relevance a common purpose, these are:

- A lasing system composed by a DFB laser diode Mitsubishi ML725B11F (with a wavelength of $\lambda=1310$ nm, with a built-in monitoring photodiode), and a custom-made conditioning circuit composed by the laser driver and a trans impedance amplifier (with a gain of 119 dB and a band-pass filter from 82Hz to 46 KHz).
- An optical system composed by a double lens configuration, one collimating lens Thorlabs C660TME-C (focal length of 2.97 mm), a MEMS Mirrorcle S4417 (diameter of 4.2 mm and an angular change of $\pm 5^\circ$), and a focusing lens Thorlabs AC254-060-C-ML (with a maximum aperture of 22.8 mm), located in the output patch to focus the target.
- A control system for the MEMS composed by a PCB connector Mirrorcle Mount-DIP.5-KMS to stablish connection with the MEMS package, an analog MEMS driver Mirrorcle BDQ PicoAmp 5.X and a Data Acquisition Board National Instruments USB-6361 OEM designed for patents and prototypes.

The entire system was designed to be packaged in two parts: The handheld device made in a 3D printer where the OFI sensor with its optical solution, the laser, and the PCB for the laser and MEMS driving are located, and a metallic base, where the DAQ and the power supply will be located. These could be seen in the Figure 27.

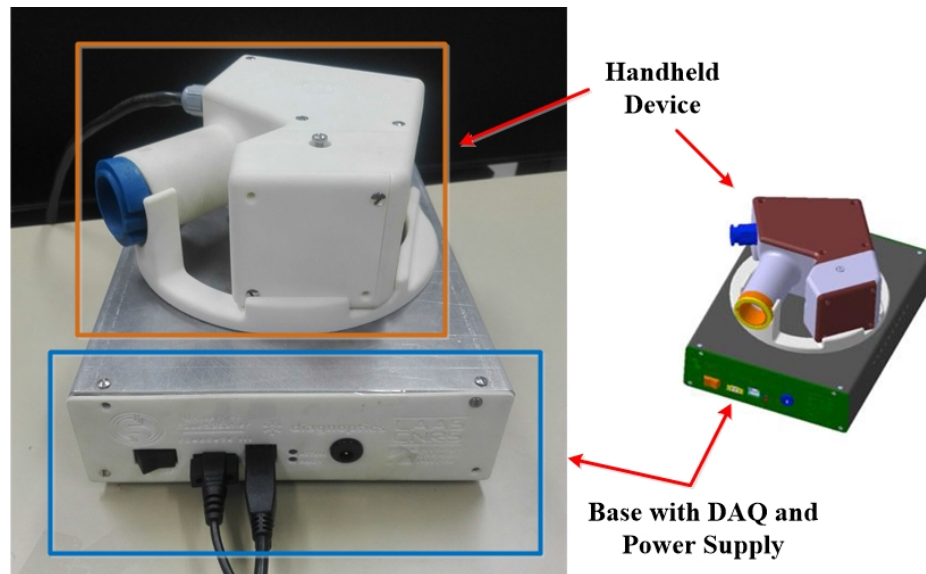


Figure 27. Diagnostics OFI Sensor with its handheld device and metallic base [3].

A. Lasing System

The lasing system is only composed by the laser diode and its conditioning circuit, The Mitsubishi ML725B11F in the worst case will have a divergence of 30° according its datasheet which is important to determine the maximum scanning area. And the conditioning circuit similarly to the case of the three axis system is used for biasing the laser diode and amplify the OFI signal provided from the monitoring photodiode.

This circuit has been placed behind the laser diode in the handheld system like it is showed in the Figure 28, and the connections were done using an armored 1.5m 14-wire cable between the base and the handheld device in order to avoid interference, since the OFI signal is captured by the DAQ located in the base, same as the power supply which is in the base.

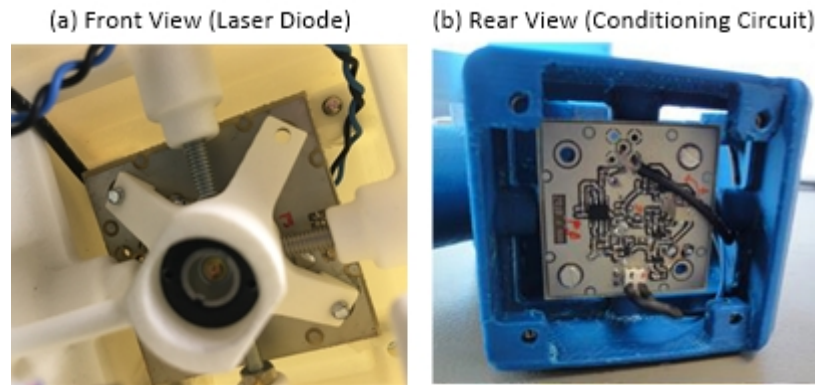


Figure 28. (a) Laser Diode and (b) Conditioning Circuit PCB placed in the handheld System.

B. Optical System

In this approach a double lens configuration was chosen for the laser beam, where the first is placed in front of the laser to collimate the beam through the steering mirror, keeping the beam width along the optical path, and then the second lens focuses on the flow target to be measured. The lens dimensioning is based in the approximations according the mirror datasheet and to obtain a 2 mm diameter collimated beam and a maximum scanning area of 20 mm x 20 mm.

Between both lens there will be located the mirror steering device Mirrorcle S4417, with a diameter of 4.2 mm. The MEMS mirror is packaged in a DIP24 chip, with a C-coated protection glass over the mirror. It has a tolerance up to $\pm 10^\circ$ and according this characteristic, it was placed in an angle of incidence of 22.5° to the normal referred the collimating lens to obtain a good scanning area, according to the Coated window over the mirror.

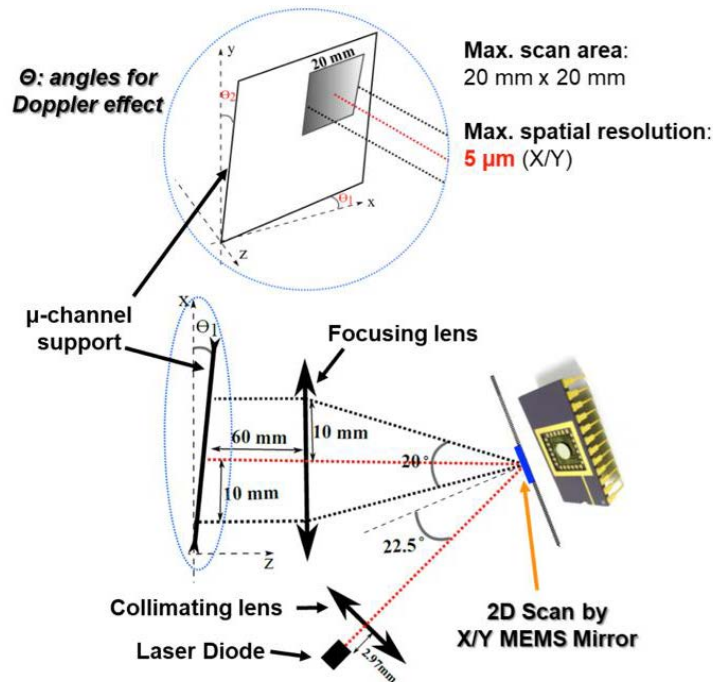


Figure 29. Optical 2D Scanning System Embedded in the handheld device [3].

In the Figure 29 it is displayed the optical configuration to achieve the best focusing over the possible scanning area, the red dotted line is the laser path when the mirror is totally centered without angle, and the black dotted line corresponds to the extremes of the angular range, in other words when the mirror is at $+5^\circ$ or -5° .

C. MEMS Control System

The tilt and tip of the MEMS Mirrorcle S4417 is controlled by an electronic part composed by three components, and thus allowing the 2D scanning over the target. These components are a PCB connector Mirrorcle Mount-DIP.5-KMS, an analog driver Mirrorcle BDQ PicoAmp 5.X and the DAQ National Instruments USB-6361. The two first are mounted in the handheld device while the DAQ is in the metallic base.

Since the MEMS is packaged in a DIP24 chip, this needs a surface to stablish connection with its controller, to accomplish this, Mirrorcle recommends to use the Mount DIP.5 KMS PCB which contains a ZIF socket of 12.5 mm of height and with a significant compactness

since the size of the DIP24 package only increment 14 mm and provide a box header connector of 10 Pins. Additionally, in this way if the mirror suffers a damage we can only change it directly to the ZIF socket without alter any structure of the prototype. This PCB is showed in the Figure 30

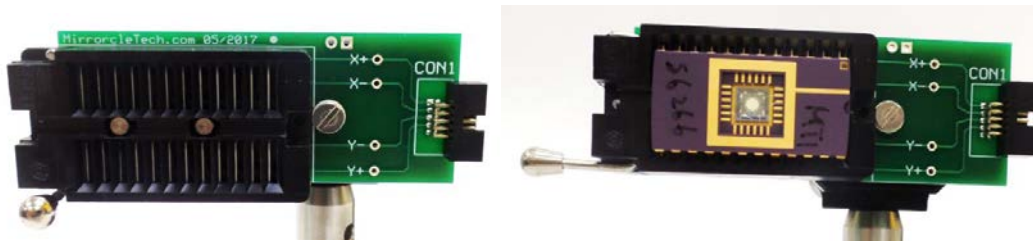


Figure 30. Mount-DIP.5-KMS PCB Connector.

The MEMS beam steering mirror is capable to perform a steering angle range from -5° to $+5^\circ$ in each direction (X/Y), thanks to the Analog Bias-Differential Quad-channel (BDQ) PicoAmp 5.X, this is possible with just the supplying voltage variation from -10V to +10V at its analog inputs. The Analog input MEMS driver count with 4 unipolar analog outputs capable to generate up to 160V to steer the mirror, it also has an input connector which could be easily interconnected with the interface PCB KMS mentioned before.

It also counts with its own Boost Controlled Converter to command X and Y rotation, the MEMS driver enable, power supply and a Low-pass Filter Control (FCLK) provided by the user for setting hardware filter cut-off.

The Bias-Differential Quad-channel (BDQ) is the proper methodology for driving MEMS mirrors, its principle consists in two strict requirements.

- All four channels are biased to 80V (V_{bias}). This is MEMS mirror origin or center point.
- Pairs of channels apply differential voltages from 0V to 160V. Mirror rotates approximately proportionally to the applied $V_{difference}$ for each axis.

Mirrorcle recommends to control and drive all these hardware, in the analog input PicoAmp Driver it is inherently implemented by adding a bias to the four output channels and forcing them as differential pairs. And that is one of the principal reasons to use this driver, since with the digital controller the methodology should be implemented by the user.

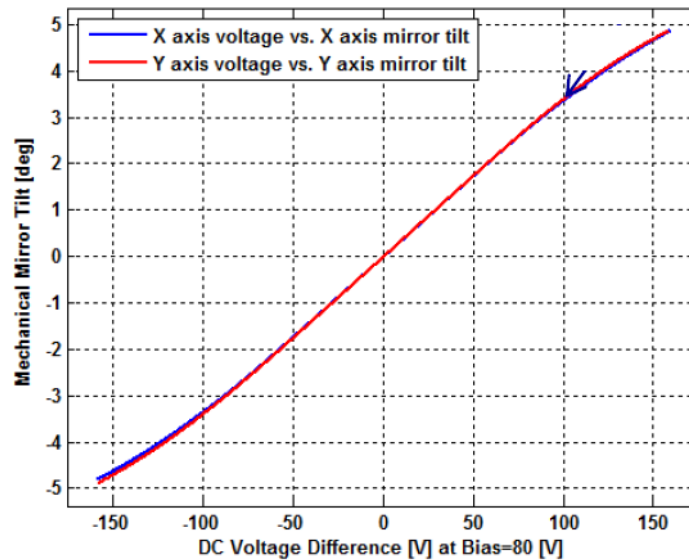


Figure 31. Control Voltage Vs Tilt Degree of the Mirror produced by the BDQ Driver.

One of the most important advantage is that the controller commands the mirror tilt angle up to reach a nearly linear behavior like it is showed in Figure 31, which is important for the scanning algorithm.

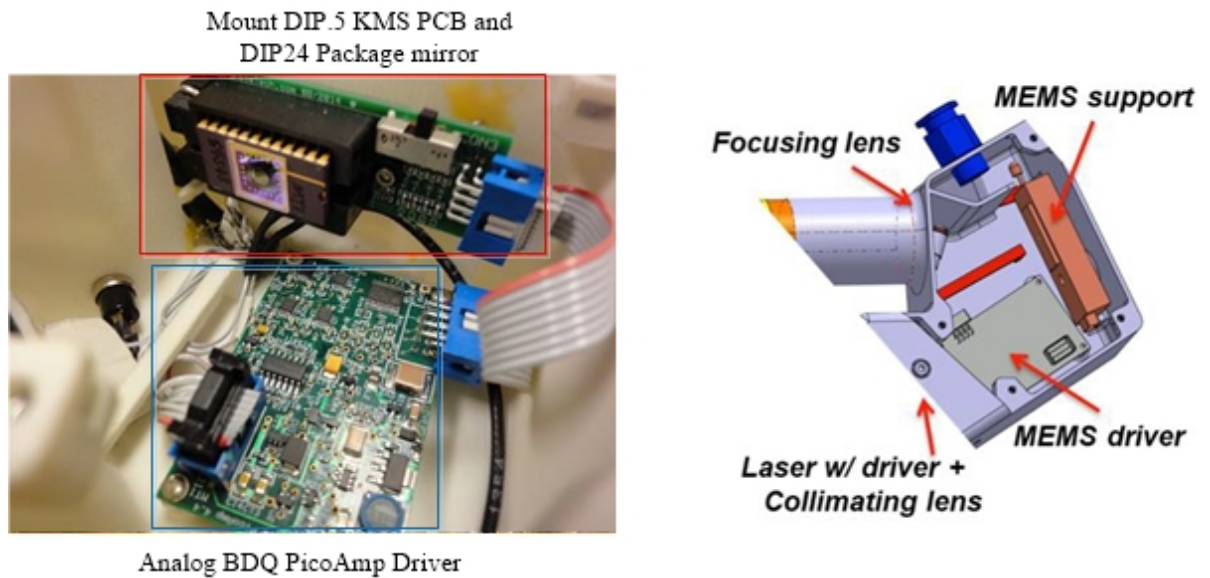


Figure 32. Handheld Device interior with placement of Beam steering mirror, PCB connector and BDQ driver.

In Figure 32 is detailed the location inside the handheld device of each one of this components, the connection are shared with the same cable used in the conditioning circuit PCB for the laser, and the optical arrangement is clearly visible using the two lenses and the mirror.

The driver is controlled using the data acquisition board National Instruments USB-6361 located in the base, with it we can generate the analog signals required to command the steering of the mirror, the digital enable signal for the driver and the clock required for the filter cut-off. The DAQ control and algorithm was originally developed in LabView® but in this work we proceeded to change the algorithm to MATLAB® with the help of the Data Acquisition Toolbox, like the previous system, and thus, taking advantage of its capabilities.

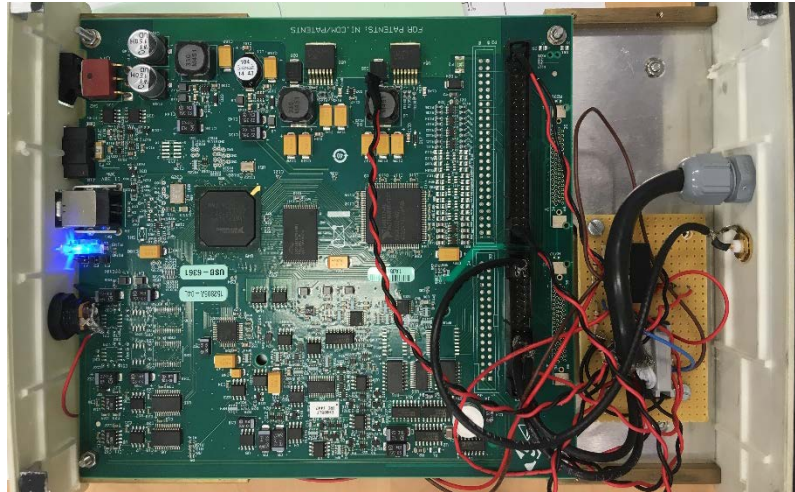


Figure 33. Inner base with the Data Acquisition Board and Power Supply.

The Figure 33 shows the DAQ NI USB-6361 placed inside the base of the system, where the connections of the power supply, signals to the driver and OFI signals are encountered. Similarly, with the case where we used the three axis system, this board has the same characteristics and it is going to be configured to take the OFI signal at 100 KHz.

3.2.2 Beam Steer Mirror Command and Data Acquisition Algorithm.

In this we have the displacement and acquisition systems linked to the same device, since the DAQ must provide the analog signals for each axis to control the mirror tilt angle, and at the same time it has to capture the OFI signal, in fact this provide us a little advantage since in MATLAB® the work performed by the DAQ could be synchronized and related to one single event.

The first step for command the mirror is to perform its initialization sequence in a specific order, and after this, we just need to change the voltage in the analog outputs associated to the axis tilt. The initialization sequence is described in Figure 34 where it is detailed step by step the necessary commands to start the mirror steer beam operation.

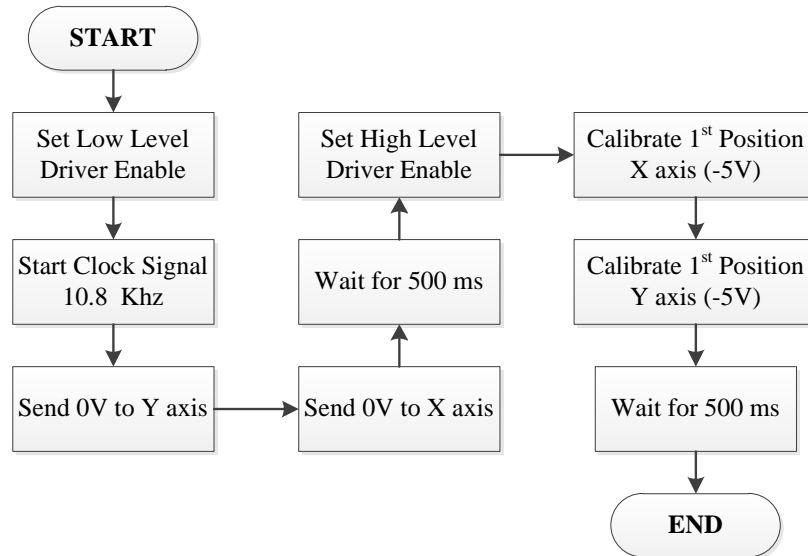


Figure 34. Flow Diagram of the Initialization Sequence of the Mirrorcle S4417.

Once the mirror is initialized, we can proceed to its command with the two analog outputs, nevertheless, we should keep the clock and enable signals activated all the time, otherwise the mirror command is interrupted, requiring the initialization sequence to be performed again.

In this approach the DAQ controls the displacement system of the laser via the tilt of the mirror, so it should be determined the angle change that could be achieved according to the characteristics of the DAQ analog output, these are linked to the point over the scanning area.

Considering linear the whole range of voltage supplied to command the mirror, we can obtain the minimum change and the voltage proportionality accorded to physical displacement over the scanning area. This could be obtained considering that the DAQ count with a resolution of 16 bits, a total range between -10V to +10V in analog outputs, and that the mirror will be controlled only using the voltage range from -5V to +5V corresponding to the extremes of the displacement of 20 mm x 20 mm. First we need to know the minimum voltage change that the DAQ could provide, this is:

$$V_{min} = \frac{V_{Range}}{DAQ_{Resolution}} = \frac{20V}{2^{16}} = 0.3055e^{-3} V \sim 0.31 mV$$

The mirror tilt responds from -5° to 5° with $-10V$ to $+10V$ respectively, this means that with the minimum voltage change that the DAQ can provide, the minimum change in angle will be:

$$\theta_{tilt_{min}} = 0.5 V_{min} = 0.000155^\circ$$

Considering that the tilt range is from -2.5° to 2.5° and that will result in the position from 0 mm to 20 mm, respectively, the minimum 2D resolution is:

$$Position_m = (0.04 \theta_{tilt_{min}} + 0.1) - (0.1) = 6.2e^{-6} m \sim 6.2 \mu m$$

The minimum spatial resolution will be $6.2 \mu m$ using our configuration, this is important to know the important changes according the 3D displacement system, however this could be improved in future with a high resolution digital to analog converter. The Table 2 summarizes the minimum characteristics obtained in our system, which establish the maximum capabilities of it.

Table 2. Minimum parameters obtained with the NI USB-6361.

DAQ Resolution	Minimum Output Voltage change	Minimum Mirror Tilt Angle change	Minimum Spatial Resolution over Scanning Area
16 bits	0.31 mV	0.000155°	$6.2 \mu m$

The minimum parameters with the MEMS in terms of spatial resolution are lower than the case of the 3D displacement system with the 3 motors, however the compactness gained is a worth trade-off since it enables the study to analyze blood perfusion and skin characteristics in the biomedical field.

Once the parameters are determined, we proceeded to develop the algorithm to perform the scanning. The first difference in this system as it was mentioned before, is that the NI DAQ

is controlling the displacement system at the same time that is capturing the OFI signal, this requires to associate the DAQ movement and acquisition to a single event in MATLAB® that when is activated is going to perform both task simultaneously, advantageously using the Data Acquisition Toolbox we can reach this.

The fixed axis like the previous case could be configured to perform the vertical or horizontal rasterization, the step change of the fixed axis works according to the minimum spatial resolution linear equation, and the continuous axis is defined by a saw tooth signal generated in MATLAB® which time duration is determined according to a desired displacement speed, since we want to achieve the same result than the 3 axis displacement system, it was decided to obtain a signal which corresponds to the speed of 6 mm/s.

Table 3. Distance Limits controlled by continuous scanning axis.

Output Voltage Limits	Distance Limits
-5 V	0 m
+5 V	0.2 m

If we want to achieve a speed of 6 mm/s, we should consider that the 20 mm of total scanning path at this speed will be reached in 3.333 seconds, so the time domain signal should have this characteristic. According to the Data Acquisition Toolbox, the queued signal duration is dependent of the scans queued and the rate defined in the output voltage channel.

$$\text{Signal duration} = \frac{\text{Scans Queued}}{\text{Rate}}$$

According to this, the length of our signal is defined by the scans queued and the rate is defined by us, for our case it was decided 1000 scans/second of rate which is enough to

accomplish a good resolution signal. With this we can define the vector length of our saw tooth signal since we know the expected time to reach the end of the path.

$$\textit{Fixed Axis Displacement [m]} = 0.02 V_{axis} + 0.1$$

$$\textit{Sawtooth Lenght [N]} = \textit{Output Rate} * \textit{time signal expected}$$

The vector length is related to the duration of the signal since it represents the number of samples queued and produced in one second in the output channel, as it was mentioned the rate should be fixed and the time duration expected of the signal is related to the displacement speed desired, these whole calculations were implemented in the algorithm previous the output and input operations.

The Figure 35 shows the algorithm sequence to perform the scanning where the NI DAQ is putted in the mode to manage both operations simultaneously, another advantage using this system is that the displacement and sensor signals measured are likely to be perfectly synchronized due to the simultaneous operation.

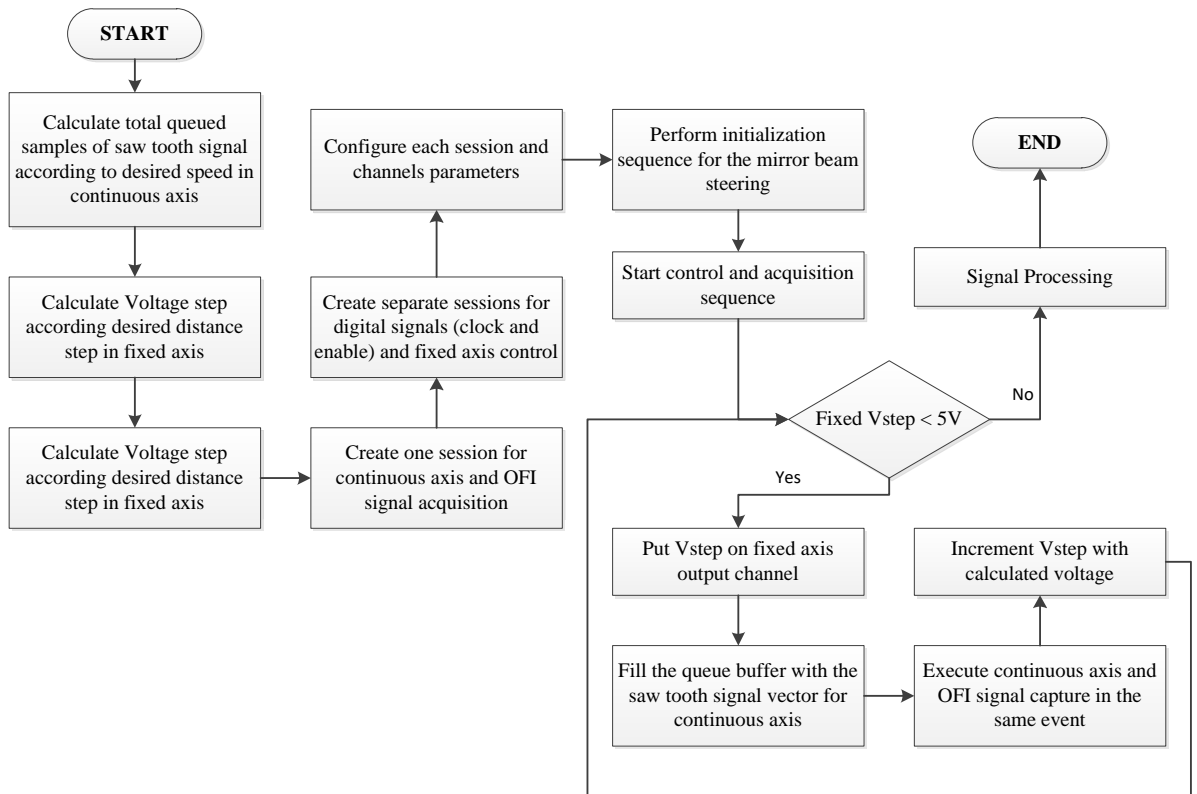


Figure 35. Flow diagram of the entire procedure for control and acquisition of the system.

The signal processing is kept similarly like the case of the three axis displacement system, based on the spectral analysis of the signal using the power spectral density (PSD), the first order moment and the segmentation of it, since the signal acquired has the same characteristic, basically the only change is the focusing and displacement systems between both, which means that the same algorithm to reconstruct the flow pattern image could be used.

3.2.3 Results.

It was done the measurement of the serpentine using the same fluid which is a dilution with a concentration of 5% of milk on water, and as was mentioned before, it will be pumped using the same hydrodynamic system. The main idea was to try to reproduce the same flow

pattern like the case of the three axis system, performing the rasterization only in the same direction as the fluid is flowing.

For this case since we cannot afford the same resolution in the fixed axis than before, it was used the fixed step of $10\ \mu\text{m}$ in the case to cover the total scanning area, and the minimum resolution available which is $6.2\ \mu\text{m}$ to measure small sections of the serpentine chip. Additionally, since the scanning area of $20\ \text{mm} \times 20\ \text{mm}$ of this device we are limited and cannot measure the whole serpentine chip.

For focusing the laser over the serpentine chip, we have placed directly the microfluidic chip in front of the handheld device, this is the highest focusing that we can achieve with this system. This procedure is displayed in Figure 36.

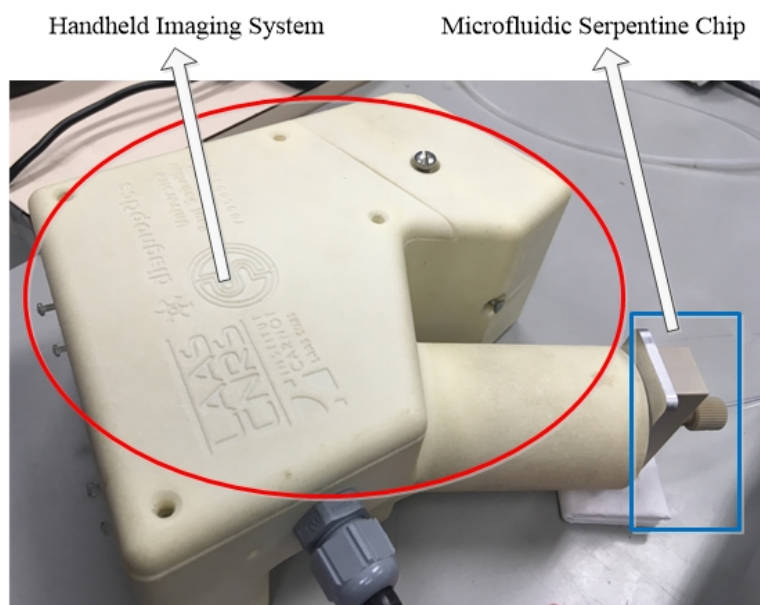


Figure 36. Focusing Over the Serpentine Chip using the Handheld System.

The first attempt to obtain the serpentine figure was done with relatively success, the Figure 37 represents the flow pattern with a clearly visibility. One of the most difficult problematics to afford in this configuration is the correct focusing over the area of interest,

since the laser wavelength is not visible and the focusing area is not so clear like the 3D axis system.

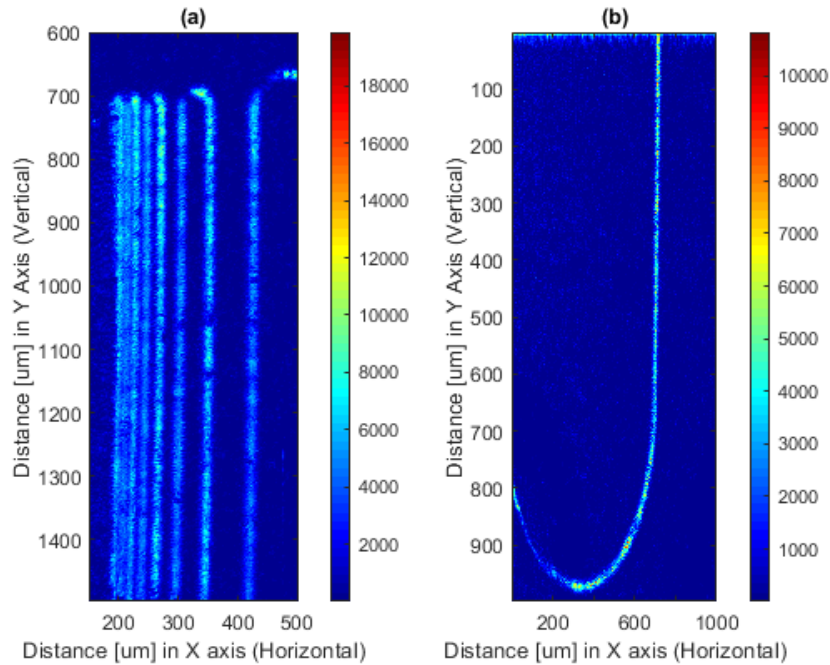


Figure 37. First measurements over the serpentine chip (a) small section of the microchannel with a fixed step of $20\ \mu\text{m}$ and a segmentation step of $10\ \mu\text{m}$.

During the acquisition using the handheld system, there were used the same displacement speed, using the algorithm and the equivalences it was reproduced the speed of 6 mm/s using the mirror steering device. The Figure 37.b shows just a small part of the serpentine with high resolution, in this image we can notice the high intensity of the flowing section.

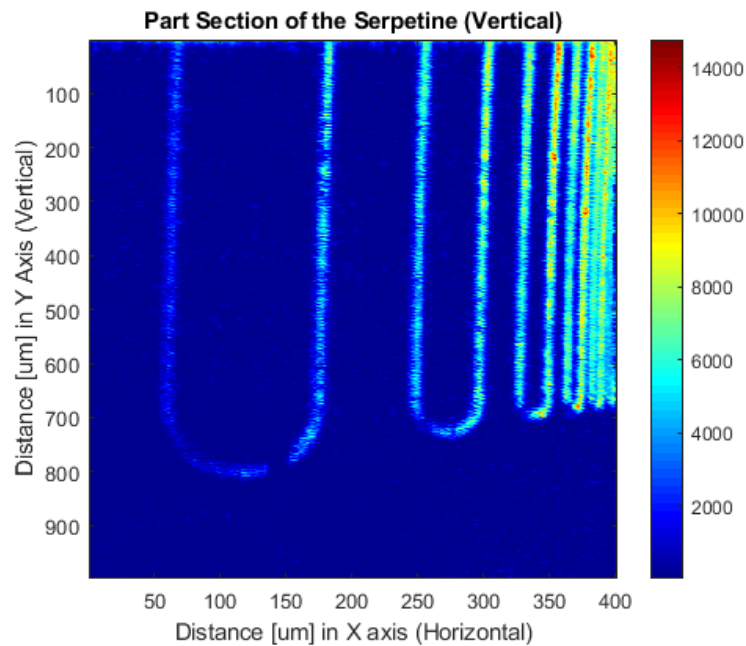


Figure 38. Section of the Serpentine taken with vertical Scanning.

At the end the results were good, since it was able to detect the flow pattern of the serpentine chip, even with this configuration. In Figure 38 it is showed the flow pattern in the serpentine form with a high covered area, during this experiment it was used the same speed and vertical step, which after 40 min results in the depicted pattern.

The Figure 38 demonstrate that this device is equally capable to detect the flow pattern with little back offs in the performance, since with this device is harder to focus in the target, meaning that the covered area is the desired because the laser is not visible for human eye.

And also the analog output is linked to the mirror resolution change, thus, the DAQ limits the resolution of the image, which could be improved with a higher resolution digital to analog converter, but at the end this will mean more cost, consequently a trade-off is kept in this handheld embedded system.

CONCLUSIONS

Regarding the state of the art of flowmetry, the imaging systems for microfluidic systems, continuous scanning technique innovates the measurement method in terms of acquisition time, signal processing and resolution, since we obtained almost the same results than using a point-to-point measurement system in terms of resolution, decreasing considerably the acquisition time.

Due to the segmentation process in the continuous scanning signal, this could mean a back-off in the final resolution of the image or even the channel recognition, however this could improve with the increment of the sampling frequency, which contributes to have more samples per segmentation, avoiding the loss of signal content.

Usually a continuous scanning imaging system is going to be limited in resolution both mechanically and electronically. In the fixed axis the displacement system will define the limits of resolution while in the continuous scanning axis, the resolution will be defined by the possible samples obtained, meaning, the sampling frequency.

Future works are planned in the OSE group at LAAS to improve the configuration of these imaging systems, in order to make them more compact and to pursue the embedded finality, which allows these to enter in the field of bio-instruments with the objective to analyze blood perfusion and diseases.

Also the signal processing could be improved in order to reduce the processing time and integrate the algorithms in the System on Chip field, where the bio-instrument will become non-dependent of too much power computing.

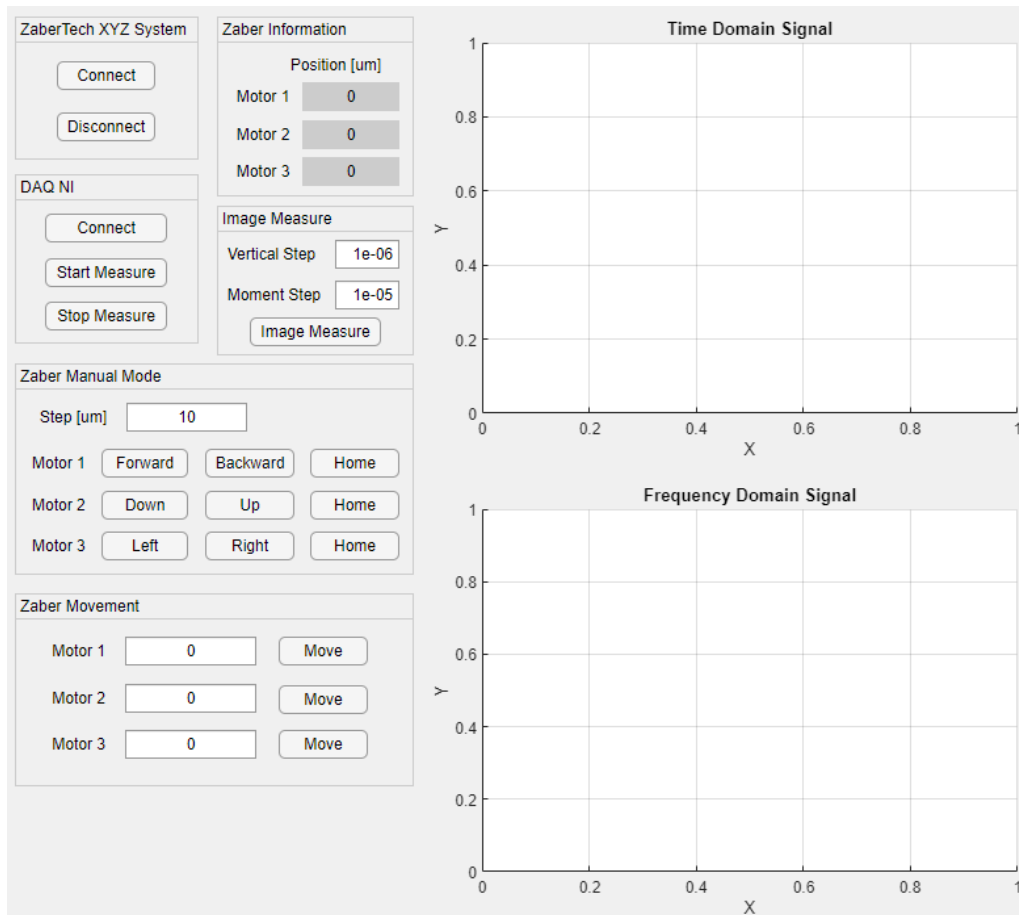
REFERENCES

- [1] L. Campagnolo, “Optical feedback interferometry sensing technique for flow measurements in microchannels,” p. 197.
- [2] E. E. Ramírez Miquet *et al.*, “Optical Feedback Interferometry: from Basics to Applications of Laser Flowmetry,” *Revista Cubana de Física*, vol. 34, pp. 48–57, Jul. 2017.
- [3] R. D. costa moreira, “Implementation of a high resolution optical feedback interferometer for microfluidics applications,” 2019.
- [4] “Optofluidics,” *Wikipedia*. 05-Mar-2019.
- [5] J. Perchoux, Y. Zhao, T. Camps, and V. Bardinal, “Optical Feedback Interferometry Flowmetry Sensor in Microfluidics Chip,” Sep. 2017.
- [6] A. Quotb, E. E. Ramírez-Miquet, C. Tronche, and J. Perchoux, “Optical Feedback Interferometry sensor for flow characterization inside ex-vivo vessel,” in *2014 IEEE SENSORS*, 2014, pp. 362–365.
- [7] R. Da Costa Moreira *et al.*, “An embedded 2D imager for microscale flowmetry based on optical feedback interferometry,” in *IEEE SENSORS 2016*, Orlando-Florida, United States, 2016, pp. 1–3.
- [8] F. F. M. de Mul *et al.*, “A Semiconductor Laser Used for Direct Measurement of the Blood Perfusion of Tissue,” *IEEE transactions on bio-medical engineering*, vol. 40, pp. 208–10, Mar. 1993.
- [9] “P. G. R. King and G. J. Steward. *New Sci.* 17, 180 (1963).,” .
- [10] P. G. R. King and G. J. Steward, “P. G. R. King and G. J. Steward, U.S. patent 3,409,370 (November 5, 1968).”
- [11] “M. Rudd. *J. Sci. Instrum.* 1, 723 (1968).”
- [12] R. Lang and K. Kobayashi, “External optical feedback effects on semiconductor injection laser properties,” *IEEE Journal of Quantum Electronics*, vol. 16, no. 3, pp. 347–355, Mar. 1980.
- [13] T. Taimre, M. Nikolić, K. Bertling, Y. L. Lim, T. Bosch, and A. D. Rakić, “Laser feedback interferometry: a tutorial on the self-mixing effect for coherent sensing,” *Adv. Opt. Photon.*, vol. 7, no. 3, p. 570, Sep. 2015.
- [14] J. Al Assad, “Analysis of Self-Mixing Moderate and Strong Feedback Regimes for Mechatronics Applications,” Oct. 2008.

- [15] “Optical feedback interferometry (OFI) | Laboratory for Analysis and Architecture of Systems.” [Online]. Available: <https://www.laas.fr/public/en/optical-feedback-interferometry-ofi>. [Accessed: 10-Jul-2019].
- [16] R. Atashkhoei, E. E. Ramírez Miquet, R. Costa, A. Quotb, S. Royo, and J. Perchoux, “Optical feedback flowmetry: Impact of particle concentration on the signal processing method,” *IEEE Sensors Journal*, vol. 18, pp. 1457–1463, Feb. 2018.
- [17] J. Perchoux *et al.*, “Current Developments on Optical Feedback Interferometry as an All-Optical Sensor for Biomedical Applications,” *Sensors*, vol. 16, no. 5, p. 694, May 2016.
- [18] Y. Zhao, “Optical feedback sensing in microfluidics: design and characterization of VCSEL-based compact systems,” p. 152.
- [19] “S. Magaletti, ‘Optical feedback interferometry for in-vivo vein detection,’ in Università Degli Studi Di Bari Aldo Moro, France, 2017.”
- [20] R. da C. Moreira, J. Perchoux, Y. Zhao, C. Tronche, F. Jayat, and T. Bosch, “Single nanoparticle flow detection and velocimetry using optical feedback interferometry,” in *2017 IEEE SENSORS*, 2017, pp. 1–3.
- [21] R. Bonner and R. Nossal, “Model for laser Doppler measurements of blood flow in tissue,” *Appl. Opt.*, vol. 20, no. 12, p. 2097, Jun. 1981.
- [22] E. E. Ramírez-Miquet, “Implementation of Optical Feedback Interferometry for Sensing Applications in Fluidic Systems,” p. 139.
- [23] L. Campagnolo, “Optical feedback interferometry sensing technique for flow measurements in microchannels,” p. 197.
- [24] R. Kliese, Y. L. Lim, E. Stefan, J. Perchoux, S. J. Wilson, and A. D. Rakić, “Rapid scanning flow sensor based on the self-mixing effect in a VCSEL,” in *2010 Conference on Optoelectronic and Microelectronic Materials and Devices*, 2010, pp. 7–8.

ÍNDICE DE ANEXOS

ANEXO A: MATLAB® Graphic user interface code



```
classdef OFI_Imager < matlab.apps.AppBase
```

```
    % Properties that correspond to app components
```

```
    properties (Access = public)
```

```
        OFI_GUI_Imager
```

```
        PanelZaber
```

```
        ZaberConnectButton
```

```
        ZaberDisconnectButton
```

```
        PanelDAQ
```

```
        DAQConnectButton
```

```
        DAQStartButton
```

```
        DAQStopButton
```

```
        PanelZaberInfo
```

```
        LabelM1PositionInfo
```

```
        LabelM2PositionInfo
```

```
        matlab.ui.Figure
```

```
        matlab.ui.container.Panel
```

```
        matlab.ui.control.Button
```

```
        matlab.ui.control.Button
```

```
        matlab.ui.container.Panel
```

```
        matlab.ui.control.Button
```

```
        matlab.ui.control.Button
```

```
        matlab.ui.control.Button
```

```
        matlab.ui.container.Panel
```

```
        matlab.ui.control.Label
```

```
        matlab.ui.control.Label
```

```

LabelM3PositionInfo      matlab.ui.control.Label
LabelM1Position          matlab.ui.control.Label
LabelM2Position          matlab.ui.control.Label
LabelM3Position          matlab.ui.control.Label
LabelPosition            matlab.ui.control.Label
PanelZaberManual         matlab.ui.container.Panel
StepumEditFieldLabel    matlab.ui.control.Label
StepumEditField          matlab.ui.control.NumericEditField
ForwardButton            matlab.ui.control.Button
BackwardButton           matlab.ui.control.Button
HomeM1Button             matlab.ui.control.Button
Motor1Label              matlab.ui.control.Label
DownButton               matlab.ui.control.Button
UpButton                  matlab.ui.control.Button
HomeM2Button             matlab.ui.control.Button
Motor2Label              matlab.ui.control.Label
LeftButton               matlab.ui.control.Button
RightButton              matlab.ui.control.Button
HomeM3Button             matlab.ui.control.Button
Motor3Label              matlab.ui.control.Label
PanelZaberMove          matlab.ui.container.Panel
MoveM1Button             matlab.ui.control.Button
MoveM2Button             matlab.ui.control.Button
MoveM3Button             matlab.ui.control.Button
Motor1EditFieldLabel    matlab.ui.control.Label
Motor1EditField          matlab.ui.control.NumericEditField
Motor2EditFieldLabel    matlab.ui.control.Label
Motor2EditField          matlab.ui.control.NumericEditField
Motor3EditFieldLabel    matlab.ui.control.Label
Motor3EditField          matlab.ui.control.NumericEditField
UIAxes                   matlab.ui.control.UIAxes
UIAxes2                   matlab.ui.control.UIAxes
ImageMeasurePanel       matlab.ui.container.Panel
VerticalStepEditFieldLabel matlab.ui.control.Label
VerticalStepEditField    matlab.ui.control.NumericEditField
MomentStepEditFieldLabel matlab.ui.control.Label
MomentStepEditField      matlab.ui.control.NumericEditField
ImageMeasureButton       matlab.ui.control.Button
end

properties (Access = private)
    myTimer % Description
end

% Callbacks that handle component events
methods (Access = private)

    % Button pushed function: ZaberConnectButton
    function ZaberConnectButtonPushed(app, event)
        global port device;

```

```

clc;
[port, device] = InitializeZaberApp(app);
end

% Button pushed function: DAQConnectButton
function DAQConnectButtonPushed(app, event)
    global daqSession channel;
    clc;
    daqData = daq.getDevices;
    daqSession = daq.createSession(daqData.Vendor.ID);
    daqSession.Rate = 2e6;
    daqSession.NumberOfScans = 4096;
    daqSession.IsContinuous = false;
    % Add Analog Channels for measuring
    channel =
addAnalogInputChannel(daqSession,daqData.ID,'ai4','Voltage');
    channel.Range = [-2, 2];
    channel.TerminalConfig = 'SingleEnded';
    daqSession.Channels
end

% Button pushed function: ZaberDisconnectButton
function ZaberDisconnectButtonPushed(app, event)
    global port;
    fclose(port);
    delete(port);
end

% Button pushed function: DAQStartButton
function DAQStartButtonPushed(app, event)
    global daqSession channel;
    app.myTimer = timer('Period',0.01, ...
                        'StartDelay',0, ...
                        'TasksToExecute',inf, ...
                        'ExecutionMode','fixedSpacing', ...
'TimerFcn',{@timerCallbackApp,app,daqSession,channel});
    start(app.myTimer);
end

% Button pushed function: DAQStopButton
function DAQStopButtonPushed(app, event)
    if(strcmp(get(app.myTimer,'Running'),'on'))
        stop(app.myTimer);
        disp('cleaned Timer');
    else
        disp('not cleaned Timer');
    end
end

```



```
    end
end

% Button pushed function: MoveM1Button
function MoveM1ButtonPushed(app, event)
    global device;
    moveZaberApp(device,1,app,0)
end

% Button pushed function: MoveM2Button
function MoveM2ButtonPushed(app, event)
    global device;
    moveZaberApp(device,2,app,0)
end

% Button pushed function: MoveM3Button
function MoveM3ButtonPushed(app, event)
    global device;
    moveZaberApp(device,3,app,0)
end

% Button pushed function: HomeM1Button
function HomeM1ButtonPushed(app, event)
    global device;
    homeZaberApp(device,1,app)
end

% Button pushed function: HomeM2Button
function HomeM2ButtonPushed(app, event)
    global device;
    homeZaberApp(device,2,app)
end

% Button pushed function: HomeM3Button
function HomeM3ButtonPushed(app, event)
    global device;
    homeZaberApp(device,3,app)
end

% Button pushed function: ForwardButton
function ForwardButtonPushed(app, event)
    global device;
    moveZaberStepApp(device,1,1,app)
end
```

```

% Button pushed function: BackwardButton
function BackwardButtonPushed(app, event)
    global device;
    moveZaberStepApp(device,1,2,app)
end

% Button pushed function: DownButton
function DownButtonPushed(app, event)
    global device;
    moveZaberStepApp(device,2,1,app)
end

% Button pushed function: UpButton
function UpButtonPushed(app, event)
    global device;
    moveZaberStepApp(device,2,2,app)
end

% Button pushed function: LeftButton
function LeftButtonPushed(app, event)
    global device;
    moveZaberStepApp(device,3,1,app)
end

% Button pushed function: RightButton
function RightButtonPushed(app, event)
    global device;
    moveZaberStepApp(device,3,2,app)
end

% Button pushed function: ImageMeasureButton
function ImageMeasureButtonPushed(app, event)
    global device daqSession channel;
    clc;
    % KILL THE MEASUREMENT TIMER
    if(strcmp(get(app.myTimer, 'Running'), 'on'))
        stop(app.myTimer);
        disp('cleaned Timer');
    else
        disp('not cleaned Timer');
    end

    % INITIAL POSITIONS
    M1pos = 19800;

```

```

M2pos = 12000;
M2pos2 = 23000;
M3pos = 27500;
M3pos2 = 23500;

moveZaberApp(device,1,app,M1pos);
moveZaberApp(device,2,app,M2pos);
moveZaberApp(device,3,app,M3pos);

% DAQ AND CONFIG OF ZABER

% ZABER
distance_x = (M3pos-M3pos2)*1e-6;
distance_y = (M2pos2-M2pos)*1e-6;
motorSpeed = 5.999857e-3;
timeDelay = distance_y/motorSpeed;

% DAQ
Fs = 100e3;
daqData = daq.getDevices;
daqSession = daq.createSession(daqData.Vendor.ID);
daqSession.Rate = Fs;
daqSession.DurationInSeconds = timeDelay;
daqSession.IsContinuous = false;
channel =
addAnalogInputChannel(daqSession,daqData.ID,'ai4','Voltage');
channel.Range = [-5, 5];
channel.TerminalConfig = 'SingleEnded';
daqSession.Channels

% PERFORM
advance = app.VerticalStepEditField.Value;
steps = round(distance_x/advance);
disp(steps)

momentStep = app.MomentStepEditField.Value;
time_distance = momentStep/motorSpeed;
samples = round(time_distance*Fs);
init_pos = 12e-3;
td = 0.04;
samples_stop = round(td*Fs);
it_still = round(samples_stop/samples);

for meas = 1 : steps
    fprintf('%d of %d \n',meas,steps);

    pos = device(3).getposition();
    position(meas,1) = 1e3*device(3).Units.nativetoposition(pos);
    pos = device(2).getposition();
    position(meas,3) = 1e3*device(2).Units.nativetoposition(pos);

```

```

fid = fopen('log.bin','w');
lh = addlistener(daqSession,'DataAvailable',@(src,
event)logData(src, event, fid));
daqSession.startBackground;

tic;
moveZaberApp(device,2,app,M2pos2);
telapsed(meas) = toc;
daqSession.stop;
delete(lh);
fclose(fid);

fid2 = fopen('log.bin','r');
[dataD,~] = fread(fid2,[2,inf],'double');
fclose(fid2);

data(:,meas) = dataD(2,:);
time(:,meas) = dataD(1,:);

segment = 1 : samples;
last_sample = round(length(data)/samples);

for j = 1 : last_sample-1
    dataAux = data(segment,meas);
    timeAux = time(segment,meas);
    %[ps,freq] = pspectrum(dataD,timeD,'power','FrequencyLimits',[0
1e6],'FrequencyResolution',5e3);
    [ps,freq] =
periodogram(dataAux,hamming(length(dataAux)),4*length(dataAux),Fs);
    %[ps, freq] =
pwelch(dataD,hamming(length(dataD)),length(dataD)/4,4*length(dataD),Fs);
    % M0(j,i) = trapz(freq,ps);
    M1(j,meas) = trapz(freq,freq.*ps);
    if (j == 1)
        dist(j,meas) = init_pos;
    elseif(j < it_still)
        dist(j,meas) = dist(j-1,meas);
    else
        dist(j,meas) = dist(j-1,meas) + momentStep;
    end
    segment = segment + samples;
end

delete log.bin

pos = device(3).getposition();
position(meas,2) = 1e3*device(3).Units.nativetoposition(pos);
pos = device(2).getposition();
position(meas,4) = 1e3*device(2).Units.nativetoposition(pos);

C = M1;

```

```

C = imgaussfilt(C,1);
imagesc(app.UIAxes,C)
colorbar(app.UIAxes);
colormap(app.UIAxes,"jet");
app.UIAxes.Title.String = 'Image Construction';
app.UIAxes.XLabel.String = 'distance';
app.UIAxes.YLabel.String = 'distance';

M3pos = M3pos - advance*1e6;
moveZaberApp(device,3,app,M3pos);
moveZaberApp(device,2,app,M2pos);
end

assignin('base','data',data);
assignin('base','time',time);
assignin('base','position',position);
assignin('base','tt',telapsed);
assignin('base','tt',M1);
end
end

% Component initialization
methods (Access = private)

% Create UIFigure and components
function createComponents(app)

% Create OFI_GUI_Imager and hide until all components are created
app.OFI_GUI_Imager = uifigure('Visible', 'off');
app.OFI_GUI_Imager.Position = [100 100 798 709];
app.OFI_GUI_Imager.Name = 'OFI Imager';

% Create PanelZaber
app.PanelZaber = uipanel(app.OFI_GUI_Imager);
app.PanelZaber.Title = 'ZaberTech XYZ System';
app.PanelZaber.Position = [19 586 140 109];

% Create ZaberConnectButton
app.ZaberConnectButton = uibutton(app.PanelZaber, 'push');
app.ZaberConnectButton.ButtonPushedFcn = createCallbackFcn(app,
@ZaberConnectButtonPushed, true);
app.ZaberConnectButton.IconAlignment = 'center';
app.ZaberConnectButton.Position = [32 53 75 22];
app.ZaberConnectButton.Text = 'Connect';

```

```

% Create ZaberDisconnectButton
app.ZaberDisconnectButton = uibutton(app.PanelZaber, 'push');
app.ZaberDisconnectButton.ButtonPushedFcn = createCallbackFcn(app,
@ZaberDisconnectButtonPushed, true);
app.ZaberDisconnectButton.IconAlignment = 'center';
app.ZaberDisconnectButton.Position = [32 14 75 22];
app.ZaberDisconnectButton.Text = 'Disconnect';

% Create PanelDAQ
app.PanelDAQ = uipanel(app.OFI_GUI_Imager);
app.PanelDAQ.Title = 'DAQ NI';
app.PanelDAQ.Position = [19 446 140 129];

% Create DAQConnectButton
app.DAQConnectButton = uibutton(app.PanelDAQ, 'push');
app.DAQConnectButton.ButtonPushedFcn = createCallbackFcn(app,
@DAQConnectButtonPushed, true);
app.DAQConnectButton.IconAlignment = 'center';
app.DAQConnectButton.Position = [23 77 93 22];
app.DAQConnectButton.Text = 'Connect';

% Create DAQStartButton
app.DAQStartButton = uibutton(app.PanelDAQ, 'push');
app.DAQStartButton.ButtonPushedFcn = createCallbackFcn(app,
@DAQStartButtonPushed, true);
app.DAQStartButton.IconAlignment = 'center';
app.DAQStartButton.Position = [23 43 93 22];
app.DAQStartButton.Text = 'Start Measure';

% Create DAQStopButton
app.DAQStopButton = uibutton(app.PanelDAQ, 'push');
app.DAQStopButton.ButtonPushedFcn = createCallbackFcn(app,
@DAQStopButtonPushed, true);
app.DAQStopButton.IconAlignment = 'center';
app.DAQStopButton.Position = [23 10 93 22];
app.DAQStopButton.Text = 'Stop Measure';

% Create PanelZaberInfo
app.PanelZaberInfo = uipanel(app.OFI_GUI_Imager);
app.PanelZaberInfo.Title = 'Zaber Information';
app.PanelZaberInfo.Position = [173 558 150 137];

% Create LabelM1PositionInfo
app.LabelM1PositionInfo = uilabel(app.PanelZaberInfo);
app.LabelM1PositionInfo.HorizontalAlignment = 'center';

```

```
app.LabelM1PositionInfo.Position = [12 68 46 16];
app.LabelM1PositionInfo.Text = 'Motor 1';

% Create LabelM2PositionInfo
app.LabelM2PositionInfo = uilabel(app.PanelZaberInfo);
app.LabelM2PositionInfo.HorizontalAlignment = 'center';
app.LabelM2PositionInfo.Position = [12 36 46 22];
app.LabelM2PositionInfo.Text = 'Motor 2';

% Create LabelM3PositionInfo
app.LabelM3PositionInfo = uilabel(app.PanelZaberInfo);
app.LabelM3PositionInfo.HorizontalAlignment = 'center';
app.LabelM3PositionInfo.Position = [12 8 46 22];
app.LabelM3PositionInfo.Text = 'Motor 3';

% Create LabelM1Position
app.LabelM1Position = uilabel(app.PanelZaberInfo);
app.LabelM1Position.BackgroundColor = [0.8 0.8 0.8];
app.LabelM1Position.HorizontalAlignment = 'center';
app.LabelM1Position.Position = [65 65 74 22];
app.LabelM1Position.Text = '0';

% Create LabelM2Position
app.LabelM2Position = uilabel(app.PanelZaberInfo);
app.LabelM2Position.BackgroundColor = [0.8 0.8 0.8];
app.LabelM2Position.HorizontalAlignment = 'center';
app.LabelM2Position.Position = [65 36 74 22];
app.LabelM2Position.Text = '0';

% Create LabelM3Position
app.LabelM3Position = uilabel(app.PanelZaberInfo);
app.LabelM3Position.BackgroundColor = [0.8 0.8 0.8];
app.LabelM3Position.HorizontalAlignment = 'center';
app.LabelM3Position.Position = [65 8 74 22];
app.LabelM3Position.Text = '0';

% Create LabelPosition
app.LabelPosition = uilabel(app.PanelZaberInfo);
app.LabelPosition.HorizontalAlignment = 'center';
app.LabelPosition.Position = [53 89 75 22];
app.LabelPosition.Text = 'Position [um]';

% Create PanelZaberManual
app.PanelZaberManual = uipanel(app.OFI_GUI_Imager);
```

```

app.PanelZaberManual.Title = 'Zaber Manual Mode';
app.PanelZaberManual.Position = [19 270 304 161];

% Create StepumEditFieldLabel
app.StepumEditFieldLabel = uilabel(app.PanelZaberManual);
app.StepumEditFieldLabel.HorizontalAlignment = 'right';
app.StepumEditFieldLabel.Position = [13 109 57 22];
app.StepumEditFieldLabel.Text = 'Step [um]';

% Create StepumEditField
app.StepumEditField = uieditfield(app.PanelZaberManual,
'numeric');
app.StepumEditField.Limits = [0 Inf];
app.StepumEditField.HorizontalAlignment = 'center';
app.StepumEditField.Position = [85 109 92 22];
app.StepumEditField.Value = 10;

% Create ForwardButton
app.ForwardButton = uibutton(app.PanelZaberManual, 'push');
app.ForwardButton.ButtonPushedFcn = createCallbackFcn(app,
@ForwardButtonPushed, true);
app.ForwardButton.Position = [66 74 66 22];
app.ForwardButton.Text = 'Forward';

% Create BackwardButton
app.BackwardButton = uibutton(app.PanelZaberManual, 'push');
app.BackwardButton.ButtonPushedFcn = createCallbackFcn(app,
@BackwardButtonPushed, true);
app.BackwardButton.Position = [145 74 68 22];
app.BackwardButton.Text = 'Backward';

% Create HomeM1Button
app.HomeM1Button = uibutton(app.PanelZaberManual, 'push');
app.HomeM1Button.ButtonPushedFcn = createCallbackFcn(app,
@HomeM1ButtonPushed, true);
app.HomeM1Button.Position = [225 74 68 22];
app.HomeM1Button.Text = 'Home';

% Create Motor1Label
app.Motor1Label = uilabel(app.PanelZaberManual);
app.Motor1Label.Position = [13 74 46 22];
app.Motor1Label.Text = 'Motor 1';

% Create DownButton

```



```

    app.DownButton = uibutton(app.PanelZaberManual, 'push');
    app.DownButton.ButtonPushedFcn = createCallbackFcn(app,
@DownButtonPushed, true);
    app.DownButton.Position = [66 42 66 22];
    app.DownButton.Text = 'Down';

    % Create UpButton
    app.UpButton = uibutton(app.PanelZaberManual, 'push');
    app.UpButton.ButtonPushedFcn = createCallbackFcn(app,
@UpButtonPushed, true);
    app.UpButton.Position = [145 42 68 22];
    app.UpButton.Text = 'Up';

    % Create HomeM2Button
    app.HomeM2Button = uibutton(app.PanelZaberManual, 'push');
    app.HomeM2Button.ButtonPushedFcn = createCallbackFcn(app,
@HomeM2ButtonPushed, true);
    app.HomeM2Button.Position = [225 42 68 22];
    app.HomeM2Button.Text = 'Home';

    % Create Motor2Label
    app.Motor2Label = uilabel(app.PanelZaberManual);
    app.Motor2Label.Position = [13 42 46 22];
    app.Motor2Label.Text = 'Motor 2';

    % Create LeftButton
    app.LeftButton = uibutton(app.PanelZaberManual, 'push');
    app.LeftButton.ButtonPushedFcn = createCallbackFcn(app,
@LeftButtonPushed, true);
    app.LeftButton.Position = [66 11 66 22];
    app.LeftButton.Text = 'Left';

    % Create RightButton
    app.RightButton = uibutton(app.PanelZaberManual, 'push');
    app.RightButton.ButtonPushedFcn = createCallbackFcn(app,
@RightButtonPushed, true);
    app.RightButton.Position = [145 11 68 22];
    app.RightButton.Text = 'Right';

    % Create HomeM3Button
    app.HomeM3Button = uibutton(app.PanelZaberManual, 'push');
    app.HomeM3Button.ButtonPushedFcn = createCallbackFcn(app,
@HomeM3ButtonPushed, true);
    app.HomeM3Button.Position = [225 11 68 22];
    app.HomeM3Button.Text = 'Home';

```

```

% Create Motor3Label
app.Motor3Label = uilabel(app.PanelZaberManual);
app.Motor3Label.Position = [13 11 46 22];
app.Motor3Label.Text = 'Motor 3';

% Create PanelZaberMove
app.PanelZaberMove = uipanel(app.OFI_GUI_Imager);
app.PanelZaberMove.Title = 'Zaber Movement';
app.PanelZaberMove.Position = [19 109 304 147];

% Create MoveM1Button
app.MoveM1Button = uibutton(app.PanelZaberMove, 'push');
app.MoveM1Button.ButtonPushedFcn = createCallbackFcn(app,
@MoveM1ButtonPushed, true);
app.MoveM1Button.Position = [201 92 68 22];
app.MoveM1Button.Text = 'Move';

% Create MoveM2Button
app.MoveM2Button = uibutton(app.PanelZaberMove, 'push');
app.MoveM2Button.ButtonPushedFcn = createCallbackFcn(app,
@MoveM2ButtonPushed, true);
app.MoveM2Button.Position = [201 55 68 22];
app.MoveM2Button.Text = 'Move';

% Create MoveM3Button
app.MoveM3Button = uibutton(app.PanelZaberMove, 'push');
app.MoveM3Button.ButtonPushedFcn = createCallbackFcn(app,
@MoveM3ButtonPushed, true);
app.MoveM3Button.Position = [201 21 68 22];
app.MoveM3Button.Text = 'Move';

% Create Motor1EditFieldLabel
app.Motor1EditFieldLabel = uilabel(app.PanelZaberMove);
app.Motor1EditFieldLabel.HorizontalAlignment = 'right';
app.Motor1EditFieldLabel.Position = [23 92 46 22];
app.Motor1EditFieldLabel.Text = 'Motor 1';

% Create Motor1EditField
app.Motor1EditField = uieditfield(app.PanelZaberMove, 'numeric');
app.Motor1EditField.Limits = [0 59000];
app.Motor1EditField.ValueDisplayFormat = '%.0f';
app.Motor1EditField.HorizontalAlignment = 'center';
app.Motor1EditField.Position = [84 92 100 22];

```

```

% Create Motor2EditFieldLabel
app.Motor2EditFieldLabel = uilabel(app.PanelZaberMove);
app.Motor2EditFieldLabel.HorizontalAlignment = 'right';
app.Motor2EditFieldLabel.Position = [23 56 46 22];
app.Motor2EditFieldLabel.Text = 'Motor 2';

% Create Motor2EditField
app.Motor2EditField = uieditfield(app.PanelZaberMove, 'numeric');
app.Motor2EditField.Limits = [0 59000];
app.Motor2EditField.ValueDisplayFormat = '%.0f';
app.Motor2EditField.HorizontalAlignment = 'center';
app.Motor2EditField.Position = [84 56 100 22];

% Create Motor3EditFieldLabel
app.Motor3EditFieldLabel = uilabel(app.PanelZaberMove);
app.Motor3EditFieldLabel.HorizontalAlignment = 'right';
app.Motor3EditFieldLabel.Position = [23 21 46 22];
app.Motor3EditFieldLabel.Text = 'Motor 3';

% Create Motor3EditField
app.Motor3EditField = uieditfield(app.PanelZaberMove, 'numeric');
app.Motor3EditField.Limits = [0 59000];
app.Motor3EditField.ValueDisplayFormat = '%.0f';
app.Motor3EditField.HorizontalAlignment = 'center';
app.Motor3EditField.Position = [84 21 100 22];

% Create UIAxes
app.UIAxes = uiaxes(app.OFI_GUI_Imager);
title(app.UIAxes, 'Time Domain Signal')
xlabel(app.UIAxes, 'X')
ylabel(app.UIAxes, 'Y')
app.UIAxes.XGrid = 'on';
app.UIAxes.YGrid = 'on';
app.UIAxes.Position = [336 358 455 337];

% Create UIAxes2
app.UIAxes2 = uiaxes(app.OFI_GUI_Imager);
title(app.UIAxes2, 'Frequency Domain Signal')
xlabel(app.UIAxes2, 'X')
ylabel(app.UIAxes2, 'Y')
app.UIAxes2.XGrid = 'on';
app.UIAxes2.YGrid = 'on';
app.UIAxes2.Position = [336 9 455 331];

```

```

% Create ImageMeasurePanel
app.ImageMeasurePanel = uipanel(app.OFI_GUI_Imager);
app.ImageMeasurePanel.Title = 'Image Measure';
app.ImageMeasurePanel.Position = [173 437 150 114];

% Create VerticalStepEditFieldLabel
app.VerticalStepEditFieldLabel = uilabel(app.ImageMeasurePanel);
app.VerticalStepEditFieldLabel.HorizontalAlignment = 'right';
app.VerticalStepEditFieldLabel.Position = [2 66 73 22];
app.VerticalStepEditFieldLabel.Text = 'Vertical Step';

% Create VerticalStepEditField
app.VerticalStepEditField = uieditfield(app.ImageMeasurePanel,
'numeric');
app.VerticalStepEditField.Limits = [0 Inf];
app.VerticalStepEditField.Position = [90 66 49 22];
app.VerticalStepEditField.Value = 1e-06;

% Create MomentStepEditFieldLabel
app.MomentStepEditFieldLabel = uilabel(app.ImageMeasurePanel);
app.MomentStepEditFieldLabel.HorizontalAlignment = 'right';
app.MomentStepEditFieldLabel.Position = [2 35 77 22];
app.MomentStepEditFieldLabel.Text = 'Moment Step';

% Create MomentStepEditField
app.MomentStepEditField = uieditfield(app.ImageMeasurePanel,
'numeric');
app.MomentStepEditField.Limits = [0 Inf];
app.MomentStepEditField.Position = [90 35 49 22];
app.MomentStepEditField.Value = 1e-05;

% Create ImageMeasureButton
app.ImageMeasureButton = uibutton(app.ImageMeasurePanel, 'push');
app.ImageMeasureButton.ButtonPushedFcn = createCallbackFcn(app,
@ImageMeasureButtonPushed, true);
app.ImageMeasureButton.Position = [25 7 100 22];
app.ImageMeasureButton.Text = 'Image Measure';

% Show the figure after all components are created
app.OFI_GUI_Imager.Visible = 'on';
end
end

% App creation and deletion

```

```
methods (Access = public)

% Construct app
function app = OFI_Imager

    % Create UIFigure and components
    createComponents(app)

    % Register the app with App Designer
    registerApp(app, app.OFI_GUI_Imager)

    if nargin == 0
        clear app
    end
end

% Code that executes before app deletion
function delete(app)

    % Delete UIFigure when app is deleted
    delete(app.OFI_GUI_Imager)
end
end
end
```

ANEXO B: MATLAB® Fuctions for Zaber-Tech Stepper Control

```

function [port,device] = InitializeZaberApp(app)
    delete(instrfind({'Port'},{'COM3'}));
    port = serial('COM3');
    set(port, 'BaudRate', 9600);
    set(port, 'DataBits', 8);
    set(port, 'FlowControl', 'none');
    set(port, 'Parity', 'none');
    set(port, 'StopBits', 1);
    set(port, 'Terminator','CR/LF');
    set(port, 'Timeout', 0.5)
    warning off MATLAB:serial:fread:unsuccessfulRead
    warning off MATLAB:serial:fgetl:unsuccessfulRead
    fopen(port);
    protocol = Zaber.Protocol.detect(port);
    try
        device = protocol.finddevices();
        fprintf('Found %d device:\n', length(device));
        for i = 1 : length(device)
            fprintf('Device %d is a %s with firmware version %f\n',
device(i).DeviceNo, device(i).Name, device(i).FirmwareVersion);
            range = device(i).getrange();
            range = 1e6*device(i).Units.nativetoposition(range);
            fprintf('device travel length is %f um.\n', range(2) - range(1));
        end
        app.LabelM1Position.Text =
num2str(1e6*device(1).Units.nativetoposition(device(1).getposition()));
        app.LabelM2Position.Text =
num2str(1e6*device(2).Units.nativetoposition(device(2).getposition()));
        app.LabelM3Position.Text =
num2str(1e6*device(3).Units.nativetoposition(device(3).getposition()));
    catch exception
        fclose(port);
        rethrow(exception);
    end
end

function homeZaberApp(device,numMotor,app)
    device(numMotor).home();
    %device(numMotor).waitforidle();
    pos = device(numMotor).getposition();
    if( numMotor == 1)
        app.LabelM1Position.Text =
num2str(1e6*device(numMotor).Units.nativetoposition(pos));
    elseif( numMotor == 2 )
        app.LabelM2Position.Text =
num2str(1e6*device(numMotor).Units.nativetoposition(pos));
    else
        app.LabelM3Position.Text =
num2str(1e6*device(numMotor).Units.nativetoposition(pos));
    end
end

function moveZaberApp(device,numMotor,app,posTarget)
    if( posTarget == 0 )

```

```

    if( numMotor == 1)
        movePos = app.Motor1EditField.Value;
    elseif( numMotor == 2 )
        movePos = app.Motor2EditField.Value;
    else
        movePos = app.Motor3EditField.Value;
    end
end
else
    movePos = posTarget;
end
targetPos = device(numMotor).Units.positiontonative(movePos/1e6);
device(numMotor).moveabsolute(targetPos);
%device(numMotor).waitforidle();
pos = device(numMotor).getposition();
if( numMotor == 1)
    app.LabelM1Position.Text =
num2str(1e6*device(numMotor).Units.nativetoposition(pos));
elseif( numMotor == 2 )
    app.LabelM2Position.Text =
num2str(1e6*device(numMotor).Units.nativetoposition(pos));
else
    app.LabelM3Position.Text =
num2str(1e6*device(numMotor).Units.nativetoposition(pos));
end
end

function moveZaberStepApp(device,numMotor,way,app)
    step = app.StepumEditField.Value;
    targetPos = device(numMotor).Units.positiontonative(step/1e6);
    % Move the Motor according to the way introduced (way=1 : advance & way=2
: return
    if(way == 1)
        device(numMotor).moverelative(targetPos);
    else
        device(numMotor).moverelative(-targetPos);
    end
    %device(numMotor).waitforidle();
    pos = device(numMotor).getposition();
    if( numMotor == 1 )
        app.LabelM1Position.Text =
num2str(1e6*device(numMotor).Units.nativetoposition(pos));
    elseif( numMotor == 2 )
        app.LabelM2Position.Text =
num2str(1e6*device(numMotor).Units.nativetoposition(pos));
    else
        app.LabelM3Position.Text =
num2str(1e6*device(numMotor).Units.nativetoposition(pos));
    end
end
end

```

ANEXO C: MATLAB® Acquisition Signal Event

```

function timerCallbackApp(~,~,app,daqSession,channel)
    [data, time] = startForeground(daqSession);
    plot(app.UIAxes,time,data);
    app.UIAxes.Title.String = 'Time Domain Data Acquisition';
    app.UIAxes.XLabel.String = 'Time [s]';
    app.UIAxes.YLabel.String = 'Amplitude (V)';
    app.UIAxes.XLim = [0 time(end)];
    app.UIAxes.YLim = [channel.Range.Min channel.Range.Max];
    app.UIAxes.XGrid = 'on'; app.UIAxes.YGrid = 'on';
    % Power Spectral Densisty
    Fs = daqSession.Rate;
    %[psdx,freq] = periodogram(data,hamming(length(data)),length(data)/8,Fs);
    [psdx,freq] = pspectrum(data,time,'power','FrequencyLimits',[0
Fs/2],'FrequencyResolution',5e3);
    %[psdx,freq] =
periodogram(data,hamming(length(data)),2.^nextpow2(100*length(data)),Fs);
    %[psdx, freq] =
pwelch(data,hamming(length(data)),length(data)/4,length(data)/8,Fs);
    plot(app.UIAxes2,freq,pow2db(psdx));
    app.UIAxes2.Title.String = 'Power Spectral Density';
    app.UIAxes2.XLabel.String = 'Frequency [Hz]';
    app.UIAxes2.YLabel.String = 'Power/Frequency [dB/Hz]';
    %app.UIAxes2.XLim = [0 100000];
    %app.UIAxes2.YLim = [-70 -10];
    app.UIAxes2.XGrid = 'on'; app.UIAxes2.YGrid = 'on';
end

```


ANEXO D: MATLAB® Code for Handheld Device Control

```

%% Program Start, Enjoy!
clc; clear;
daqreset;
%% Voltage step for fixed axis computation
fixAxisStep = 25e-6; % Fixed axis step advance (6.2e-6
min)
voltStep = 500*fixAxisStep; % Voltage step for fixed axis
fixed1 = 10e-3; % Fixed Axis start point [m]
fixed2 = 20e-3; % Fixed Axis end point [m]
vStart = 500*fixed1-5; % Fixed Axis Volt start point [V]
vEnd = 500*fixed2-5; % Fixed Axis Volt end point [V]
%% Signal construction according to speed and distance desired
aoRate = 100e3; % An Out rate 1000 scans/sec
initDistance = 0; % Initial point of cont. axis
endDistance = 15e-3; % Continuous axis path in m
targetSpeed = 6e-3; % Continuous axis speed in m/s
totalDist = endDistance - initDistance; % Whole path crossed cont axis
signalTime = totalDist/targetSpeed; % time duration of signal
signalLength = signalTime*aoRate; % Length required for time
t = linspace(0,signalTime,signalLength); % Linear vector for signal time
signalStart = 500*initDistance-5;
signalEnd = 500*endDistance-5;
contSignal = linspace(signalStart,signalEnd,signalLength); % Sawtooth signal
for scan
%% Analog input parameters
Fs = 100e3; % Sampling Frequency
%% Initialize Session and channels for the DAQ
% Initialize Each Session for each purpose
daqData = daq.getDevices
% Analog Input and X axis Output
ai_aox_Session = daq.createSession(daqData.Vendor.ID);
ai_aox_Session.Rate = Fs;
ai_aox_Session.DurationInSeconds = signalTime;
ai_aox_Session.IsContinuous = false;
% Analog Output Y Axis
aoySession = daq.createSession(daqData.Vendor.ID);
aoySession.Rate = aoRate;
aoySession.IsContinuous = false;
% Digital Output
doSession = daq.createSession(daqData.Vendor.ID);
% Clock signal
clkSession = daq.createSession(daqData.Vendor.ID);
clkSession.IsContinuous = true;
%% Configuration of DAQ channels
% Configure Channels according to each session
% Add Analog Input Channel for measuring OFI Signal
addAnalogInputChannel(ai_aox_Session,daqData.ID,'ai0','Voltage')
ai_aox_Session.Channels(1,1).Range = [-5, 5];
ai_aox_Session.Channels(1,1).TerminalConfig = 'SingleEnded';
ai_aox_Session.Channels(1,1).Name = 'OFI Signal';
% X Axis channel
addAnalogOutputChannel(ai_aox_Session,daqData.ID,'aol','Voltage')
ai_aox_Session.Channels(1,2).Range = [-10, 10];
ai_aox_Session.Channels(1,2).Name = "X Axis Command";

```

```

% Add Analog Output for Control Mirror Steer
% Y Axis channel
addAnalogOutputChannel(aoySession,daqData.ID,'ao0',"Voltage")
aoySession.Channels.Range = [-10, 10];
aoySession.Channels.Name = "Y Axis Command";
% Add Digital Output for Enable Mirror Driver
addDigitalChannel(doSession,daqData.ID,'port0/line0','OutputOnly')
doSession.Channels.Name = 'Enable Driver';
% Add Counter Output Channel for Clock
addCounterOutputChannel(clkSession,daqData.ID,'ctr0','PulseGeneration')
clkSession.Channels.Frequency = 10.8e3;
clkSession.Channels.DutyCycle = 0.5;
clkSession.Channels.InitialDelay = 0.5;
clkSession.Channels.Name = 'Clock Mirror';
%% Mirror Initialization Sequence
% 1st sequence
outputSingleScan(doSession,0);           % Enable OFF
startBackground(clkSession);             % Start Clock
outputSingleScan(aoySession,0);         % put Y axis to 0V
outputSingleScan(ai_aox_Session,0);     % put X axis to 0V
pause(0.5);
% 2nd sequence
outputSingleScan(doSession,1);          % Enable ON
% 3rd Sequence
outputSingleScan(ai_aox_Session,-5);    % put X axis to -5V
outputSingleScan(aoySession,-5);       % put Y axis to -5V
pause(0.5);
%% Data Acquisition
% Moving with signal generation
meas = 1;
for i = vStart : voltStep : vEnd
    fprintf('%d of %d \n',meas,round((vEnd-vStart)/voltStep));
    outputSingleScan(aoySession,i);
    queueOutputData(ai_aox_Session,contSignal');
    [data(:,meas),time(:,meas)] = startForeground(ai_aox_Session);
    meas = meas + 1;
end

```

ANEXO E: MATLAB® Code for Imaging Construction

```

%%
clc;
clear M0 M1;
%%
% Define Start Parameters
Fs = 100e3;
distance = 10e-6;
speed = 6e-3;
time_distance = distance/speed;
samples = round(time_distance*Fs);
last_sample = round(length(data)/samples);
dist = zeros(last_sample-1,length(data(1,:)));
M0 = zeros(last_sample-1,length(data(1,:)));
M1 = zeros(last_sample-1,length(data(1,:)));
%%
for i = 1 : length(data(1,:))
    fprintf('%d of %d \n',i,length(data(1,:)));
    segment = 1 : samples;
    for j = 1 : last_sample
        dataD = data(segment,i);
        timeD = time(segment,i);
        %[ps,freq] = pspectrum(dataD,timeD,'power','FrequencyLimits',[0
1e6],'FrequencyResolution',5e3);
        [ps,freq] =
periodogram(dataD,hamming(length(dataD)),4*length(dataD),Fs);
        %[ps, freq] =
pwelch(dataD,hamming(length(dataD)),length(dataD)/4,4*length(dataD),Fs);
        M0(j,i) = trapz(freq,ps);
        M1(j,i) = trapz(freq,freq.*ps);
        if (j == 1)
            dist(j,i) = 0;
        else
            dist(j,i) = dist(j-1,i) + distance;
        end
        segment = segment + samples;
    end
end
%%
figure;
C = M1';
C = imgaussfilt(C,1);
imagesc(C')
colorbar;
colormap Jet;

```